University of Alberta

Mineral Deposit Modeling with Pseudo-Genetically Constructed Training Images

by

Jeffery Brian Boisvert ©

A thesis submitted to the Faculty of Graduate Studies and Research
in partial fulfillment of the requirements for the degree of

Master of Science
in
Mining Engineering

Department of Civil and Environmental Engineering

Edmonton, Alberta
Spring 2007

Library and Archives Canada

Published Heritage Branch

395 Wellington Street
Ottawa ON K1A 0N4
Canada

Bibliothèque et Archives Canada

Direction du Patrimoine de l'édition

395, rue Wellington
Ottawa ON K1A 0N4
Canada

Your file Votre référence
ISBN: 978-0-494-29938-8
Our file Notre référence
ISBN: 978-0-494-29938-8

NOTICE:
The author has granted a non-exclusive license allowing Library and Archives Canada to reproduce, publish, archive, preserve, conserve, communicate to the public by telecommunication or on the Internet, loan, distribute and sell theses worldwide, for commercial or non-commercial purposes, in microform, paper, electronic and/or any other formats.

The author retains copyright ownership and moral rights in this thesis. Neither the thesis nor substantial extracts from it may be printed or otherwise reproduced without the author's permission.

AVIS:
L'auteur a accordé une licence non exclusive permettant à la Bibliothèque et Archives Canada de reproduire, publier, archiver, sauvegarder, conserver, transmettre au public par télécommunication ou par l'Internet, prêter, distribuer et vendre des thèses partout dans le monde, à des fins commerciales ou autres, sur support microforme, papier, électronique et/ou autres formats.

L'auteur conserve la propriété du droit d'auteur et des droits moraux qui protège cette thèse. Ni la thèse ni des extraits substantiels de celle-ci ne doivent être imprimés ou autrement reproduits sans son autorisation.

In compliance with the Canadian Privacy Act some supporting forms may have been removed from this thesis.

While these forms may be included in the document page count, their removal does not represent any loss of content from the thesis.

Conformément à la loi canadienne sur la protection de la vie privée, quelques formulaires secondaires ont été enlevés de cette thèse.

Bien que ces formulaires aient inclus dans la pagination, il n'y aura aucun contenu manquant.

Canada

Don't cry because it's over, smile because it happened.
Dr. Seuss

Abstract

Multiple point statistics has surfaced as the answer to many of the limitations of traditional variogram based facies modeling. Research has explored implementation difficulties facing a successful application of multiple point statistics; however, there are no readily available, geologically realistic training images for mineral deposits. Various sources of training images are considered including: using data sets as training images; generating training images for vein type deposits from pseudo genetic mimicking of the geological processes that formed the deposit; and, using currently available geostatistical techniques to generate the desired nonlinear features observed in weathered deposits.

The selection of a training image for use in multiple point statistics can be difficult. Often, there is little objective evidence to select a specific training image. A methodology to rank training images based on a multiple point statistical comparison to exploration data is presented as objective support for selecting an appropriate training image.

Acknowledgements

Without the support and guidance of Clayton Deutsch this thesis would not have been possible. I would also like to thank all other members of the Centre for Computational Geostatistics for their help throughout this process. I would especially like to thank John Manchuk for the countless hours of discussion and programming support.

My father has also been a source of consistent support throughout the many years I have spent in school, for his help I am grateful.

Most importantly, I would like to thank the love of my life for her understanding and support of the many hours that were spent during working on this thesis. She has always encouraged me to follow my dreams and for that I can not thank her enough.

Table of Contents

CHAPTER 1: INTRODUCTION **1**

1.1 Background **3**

1.1.1 Stationarity 4

1.1.2 Variogram Use and Limitations 4

1.1.3 Multiple Point Statistics 7

1.1.4 Using Multiple Point Statistics 10

1.1.5 Vein Deposits 11

1.1.6 Weathered Deposits 12

CHAPTER 2: DATA FOR TRAINING IMAGES **16**

2.1 Data Sets as TIs **16**

2.1.2 Anglo American Data 16

2.1.3 Walker Lake Data 18

2.1.4 Discussion 20

2.2 Simulated Data **20**

2.2.1 Training Image Library 20

2.2.2 Scanned Images 21

CHAPTER 3: PROCESS BASED VEIN TYPE TRAINING IMAGES **23**

3.1 Proposed Methodology **23**

3.1.1 Step 1: Fracture Model Generation 24

3.1.2 Step 2: Permeability 25

3.1.3 Step 3: Flow Rate Calculation 25

3.1.4 Step 4: Locate Veins 27

3.2 Example **27**

3.2.1 Steps 1 and 2 – Fracture Model and Permeability 28

3.2.2 Step 3 – Flow Rate Calculation 28

3.2.3 Step 4 - Locate Veins 30

3.2.4 Discussion 32

CHAPTER 4: WEATHERED DEPOSIT TRAINING IMAGES 35

4.1 Proposed Methodology 35

4.1.1 Step 1: Synthetic Drill Hole Data for Control Points 35

4.1.2 Step 2: Assigning Conditioning Data for SGS 36

4.1.3 Step 3: SGS 38

4.1.4 Step 4: Smoothing 39

4.2 Example 39

4.2.1 Steps 1 and 2: Synthetic Drill Hole Data 39

4.2.2 Steps 3: SGS 40

4.2.3 Step 5: MAPS Smoothing 41

4.3 Sensitivity 42

4.4 Discussion 45

CHAPTER 5: SELECTING APPROPRIATE TRAINING IMAGES 47

5.1 Proposed Methodology 48

5.1.1 Using Runs to Select TIs 48

5.1.2 Using the Multiple Point Histogram to Select TIs 51

5.1.3 Example: Selecting Vein Type TIs for Pseudo Drillhole Data 52

5.1.4 Discussion 55

5.2 Case Study: Chevron Data 55

5.2.1 Selecting TIs for Chevron Data 55

5.2.2 Discussion: Using MPS to Select TIs 58

5.2.3 Realization Ranking with MPS 59

5.2.4 Generating Realizations: SNESIM 60

5.2.5 Generating Realizations: SIS 60

5.2.6 Comparing Geostatistical Realizations to TIs 61

5.2.7 Discussion: Using MPS to Rank Realizations 63

CHAPTER 6: CONCLUSIONS AND FUTURE WORK **66**

6.1 Conclusions **66**

6.2 Future work **68**

BIBLIOGRAPHY **70**

List of Tables

3-1: Effect of input parameters on vein type training images. 31

4-1: Sensitivity of weathered TIs to input parameters. 43

List of Figures

1-1: Fracture model used to generate vein type TIs. 6

1-2: Conditioned SIS and MPS models from a vein type TI. 6

1-3: Calculating the distribution of runs for a drill hole. 7

1-4: Distribution of runs example. 8

1-5: All possible arrangements of a 4 point configuration with two categories. 8

1-6: Example image to calculate the multiple point histogram. 9

1-7: Multiple point histogram of the image in Figure 1-6. 9

1-8: Three possible multiple point templates. 10

1-9: Inferring conditional probabilities at an unknown location using Bayes' law. 11

1-10: Types of basic folding and faulting. 12

1-11: Typical horizon of a weathered deposit. 14

1-12: Interpretation of a laterite profile at La Caridad, Sonora, Mexico. 15

1-13: Interpretation of a laterite profile near Poços de Caldas, Brazil. 15

1-14: Photograph of an iron bauxite contact on a mined bench. 15

2-1: Location of samples in the Anglo American dataset. 17

2-2: Basic statistics for the Anglo American dataset. 18

2-3: Maps of the Walker Lake variables. 19

2-4: Histograms and scatter plot of the Walker Lake variables. 19

2-5: Example fluvial TIs from Pyrcz and Deutsch (2003). 21

2-6: Example deepwater TIs from Pyrcz and Deutsch (2003). 22

2-7: Using a scanned image as a TI for a bedded deposit. 22

3-1: Typical horizontal slice of the Whiteshell fracture model. 24

3-2: Pressure gradient in the x-direction. 25

3-3: Calculation of the total flow rate in a single block in a 2D model. 26

3-4: Calculation of the total flow rate in a block for three pressure gradients. 27

3-5: View of the fracture model used to generate TIs. 28

3-6: Typical slice of pressure with a horizontal pressure gradient. 29

3-7: Total flow in the model for pressure gradients in the x and y directions. 29

3-8: Combined flow in the model for pressure gradients in the x and y directions. 30

3-9: Initial fault model and a TI generated from the fault model. 32

3-10: West Lake gold mine, Mount Uniacke, Nova Scotia compared to a TI. 33

3-11: Louvicourt Goldfield deposit at Val d'Or in Quebec compared to a TI. 33
4-1: Coarse grid for simulation of the initial depth of the boundary. 36
4-2: Example drill hole showing assignment of positive and negative values. 37
4-3: Adding a skin of positive and negative conditioning data. 37
4-4: Adding a layer of positive and negative conditioning data to the model. 38
4-5: Initial control points for the depth to the boundary. 39
4-6: Drill holes assigned positive and negative values. 40
4-7: Simulated positive and negative values. 41
4-8: Simulated values with a threshold of 0 applied to define the boundary. 41
4-9: Simulated values with a threshold of 0 applied to define the boundary, smoothed. 42
4-10: Effect of increasing the variogram range on weathered TIs. 44
4-11: Effect of different conditioning data options on the weathered TIs. 44
4-12: Effect of different smoothing options on weathered TIs. 45
4-13: Comparison of a TI with a weathered contact. 46
5-1: The difference between two runs distributions. 48
5-2: Effect of reducing the number of facies in a TI. 50
5-3: Comparing two multiple point histograms. 52
5-4: A typical slice of the fault model showing the location of the five TIs. 53
5-5: Considering three TIs as the one dimensional statistics in three directions. 53
5-6: Comparing the runs distribution to using the multiple point histogram. 54
5-7: Three TIs received from Chevron. 56
5-8: Runs distribution for the Chevron TIs. 56
5-9: Comparing the TIs to the Chevron well data. 57
5-10: Cross plot of the score received by each TI. 57
5-11: 32 wells from the highest and lowest ranked TIs, taken as columns of the TI. 58
5-12: Cross sections of Chevron TI #3. 59
5-13: Typical SNESIM (Strebelle, 2002) realization. 60
5-14: Typical SIS realization. 61
5-15: Comparing the variogram from the TI and one typical SIS realization. 61
5-16: Ranking realizations based on the runs distribution. 62
5-17: Ranking realizations based on the multiple point histogram. 63
5-18: Comparing ranking measures. 63
5-19: Ranking the SNESIM realizations using the multiple point histogram. 64
5-20: Cross sections of ranked SNESIM realizations and the parent TI. 65

List of Symbols

$\mathbf{h}$	distance or lag vector
$\mathbf{u}$	a location in space
$Z(\mathbf{u})$	a random variable
$2\gamma(\mathbf{h})$	variogram at a lag $\mathbf{h}$
$C(\mathbf{h})$	covariance between points separated by a distance $\mathbf{h}$
E	expected value
σ^2	variance
λ_i	weight for the i^{th} data point
P(A)	the probability that event A will occur
P(A∩B)	the probability that event A and event B will occur
P(A|B)	the probability that event A will occur given event B
a	range or distance parameter
ah1	range parameter in the horizontal direction with the maximum continuity
ah2	range parameter in the horizontal direction with the minimum continuity
sph	a spherical variogram structure
C	contribution factor for a variogram structure
Q	flow rate
A	area
K	hydraulic conductivity
Δp	change in pressure
L	length of flow
g	acceleration constant due to gravity
ρ	density
NTG	net to gross ratio
NTS	not to scale
SGS	sequential Gaussian simulation
SIS	sequential indicator simulation
SNESIM	single normal equation simulation
TI	training image

Chapter 1: Introduction

Grade estimation requires a geological model that defines the extension, shape and distribution of geological units. These units are characterized by unique lithology, alteration and mineralogy that determine the behavior of the geological unit. Spatial continuity varies from one unit to another and is taken into account by creating a facies model. A facies model is a block model that is populated with integer codes representing different rock types such as: vein/non-vein; high/low grade; and fresh/oxidized. Each facies has unique properties and is often modeled independently.

Several approaches exist to create the facies model. Deterministic modeling is the most common approach (Duke and Hanna, 2001; Sinclair and Blackwell, 2002), however several geostatistical methods have become available for stochastic simulation of the geology (Deutsch, 2002; Armstrong et al., 2003). Conventional geostatistical techniques are often limited to using the linear relationship between data, commonly represented by variogram models.

The motivation to use multiple point statistics (MPS) to generate the facies model is that traditional geostatistical techniques often generate rock type models that do not capture the complex geologies seen in mineral deposits. Because traditional techniques can only capture the linear relationship between data in the form of the variogram, any nonlinear features of a deposit cannot be reproduced in the facies model. Multiple point statistics can be used to generate facies models that contain the complex nonlinear features seen in mineral deposits (Journel, 2004). See Section 1.1.2 for an example of features that are not reproduced using traditional geostatistical techniques but are reproduced using multiple point statistics. It is also possible to use object based modeling to place geological features, such as veins, into a facies model but it is often difficult to condition these models to data. The solution is to generate unconditional facies models that contain the desired geological features and then use multiple point statistics to reproduce these features in a facies model conditioned to the available data.

Multiple point statistics can reproduce the nonlinear features in a deposit as it considers the relationship between multiple data points (Guardiano and Srivastava, 1993). Analysis of data has been confined to the variogram because multiple point statistics require a much larger number of exploration data which are often expensive to obtain. This problem can be solved by using densely drilled production samples from production data (Ortiz and Deutsch, 2004) or by using a training image (TI) (Strebelle and Journel, 2000). The availability of dense sampling is not realistic in the early stages of mining and can only occur once production has begun. TIs appear as the primary solution to obtain the statistics required for a multiple point analysis in the early stages of mining.

A TI is a facies model that is exhaustively populated by the rock types of interest. This TI contains the complex geological features of a mineral deposit but is not conditioned to the exploration data. It is assumed that the TI has the same multiple point statistics of the deposit of interest This is analogous to assuming that the TI contains the same complex geological features of the deposit of interest. A large TI ensures that statistics between any number of points can be obtained.

Once a TI has been created that represents the geological features of a deposit, a multiple point simulation algorithm can be used to reproduce these features and condition the facies model to the available data. These techniques are beyond the scope of this thesis, see section 1.1.4 for a list of simulation algorithms available.

The use of multiple point statistics is limited by the computational effort required to generate the facies model and the ability of the multiple point algorithm to reproduce the desired geological features in the conditioned models. Solutions to these problems are becoming available, such as those suggested by Zhang, Switzer and Journel (2004); Liu *et al* (2004); and Arpat and Caers (2004). Even as these difficulties are overcome, multiple point statistical methods are still dependent on a TI that is representative of the deposit of interest, just as traditional variogram methods are dependent on the variogram model.

A problem facing the mining industry is that there are currently no TIs readily available for a given type of deposit. There are TIs appropriate for fluvial and deepwater oil reservoirs (Pyrcz and Deutsch, 2003); however, the mining industry is limited to using data from extensively sampled areas. If mining geostatisticians wish to use multiple point statistics to model their deposit, they must seek a mined out area or a similar deposit that has been extensively sampled and use the statistics from that area. This has drawbacks such as the difficulty in finding a deposit that has been both extensively sampled and is similar to the deposit of interest, as well as the reluctance of many companies to share their production data. Regardless of these drawbacks, using real data as a TI has the benefit of ensuring geological realism. A series of exhaustive data sets are presented in this thesis that could be used as TIs.

A practical solution to the lack of actual data for a specific mineral deposit is to create computer programs that can generate TIs given specific information about the area of interest. A methodology is proposed to create TIs for vein type deposits by modeling the formation process of veins. Recall that these TIs are unconditioned; thus, the methodology can be applied to any vein type deposit to generate appropriate TIs. The methodology begins with a fracture model that is representative of the deposit of interest. Because TIs are unconditioned, this fracture model does not have to be conditioned to the actual fractures of the deposit of interest. Rather it only needs to have the correct characteristics of the deposit such as correct fracture spacing, orientation, prevalence, and density. This type of information is often known about the deposit during the exploration stage. Once the fracture model is generated the proposed methodology can be implemented by the practitioner to generate realistic TIs for the deposit. Moreover, a methodology to create TIs for weathered deposits using sequential Gaussian simulation

(SGS) is also presented. In this case, SGS is used to generate a realistic boundary between weathered layers. Generating TIs for different mineral deposit will allow the mining industry to apply multiple point simulation to generate facies models that capture the complex features of mineral deposits.

Many realistic TIs can be generated using these pseudo genetic processes. Multiple unconditioned fracture models could be created that would generate numerous TIs. It is often difficult to select the one TI that best represents the area of interest. The choice of TI is subjective to some extent. It is proposed that the multiple point statistics of TIs be compared to the multiple point statistics of the exploration data to objectively identify the TIs that are most representative of the exploration data. Two different multiple point statistics are used to rank TIs. This provides an objective tool to further narrow the search for the most appropriate TI.

The methodology proposed to rank TIs based on their similarity to exploration data can be extended to ranking geostatistical realizations based on their similarity to their parent TI. Once realizations have been generated using a multiple point algorithm they can be compared to their parent TI to assess how well the multiple point algorithm reproduced the nonlinear features of the TI.

1.1. Background

Facies models are critical to dealing with rock types that display different characteristics. This is the issue of stationarity; different rock types have different directions of anisotropy, means, continuity, distributions, etc. A brief discussion of stationarity will highlight the need for the facies model.

Geostatisticians are becoming increasing concerned that the facies models generated using traditional variogram based techniques do not contain the geological features of the rock types they represent. The relative simplicity of the variogram is attractive but any information beyond the linear relationship between data is ignored. A description of the variogram is given to highlight these limitations. Moreover, an example of a facies model generated using a variogram based technique and a facies model generated using a multiple point algorithm shows the advantages of considering multiple point statistics.

A brief overview of the geological formation of veins and weathered deposits will give the reader the necessary background to judge the effectiveness of the proposed TIs in mimicking the geology of actual deposits. Images of vein and weathered deposits will also serve as the bases for a visual assessment of the TIs.

Generating a TI is only the initial step in estimating or simulating with multiple point techniques. Once a TI has been selected, the multiple point statistics from that TI must be reproduced in a set of realizations. These statistics can never be duplicated exactly or the resulting simulations would be identical to the TI; however, the multiple point statistics of the realizations should be as close as possible to the TI while honouring the

available data for the deposit of interest. The basics of what multiple point statistics are and some methods for using them to generate conditional realizations will be given.

1.1.1. Stationarity

The choice of stationarity assumes that the area considered has the same statistical properties throughout. First order stationarity assumes that the mean and variance of the variable of interest is constant throughout the domain. Second order stationarity assumes that the covariance between data is constant throughout the domain or that the variogram used is constant throughout the domain.

Different rock types often have a different mean, variance, or covariance. If this is the case, the assumption of stationarity is violated. There are a variety of solutions to modeling domains that are not stationary. If only the mean is violating the stationarity assumption and the covariance is constant throughout the domain, a trend model can be used to remove the non stationary behavior (Isaaks and Strivastava, 1989). However, if the variance or covariance changes throughout the domain, it is common to divide the domain into smaller domains until all are stationary. Modeling is then done independently in each smaller domain. One method to define domains is to generate a facies model to separate the rock types such that each rock type is stationary and can be modeled separately. This is the motivation for generating a facies model.

1.1.2. Variogram Use and Limitations

The variogram is commonly used to define the relationship between two locations in space separated by a distance **h**. The two locations are defined as **u** and **u** + **h**, by definition the variogram (2γ) is:

$$\begin{aligned} 2\gamma(\mathbf{h}) &= E\left\{\left[Z(\mathbf{u})-Z(\mathbf{u}+\mathbf{h})\right]^2\right\} \\ &= E\left\{\left[Z(\mathbf{u})\right]^2\right\}-2E\left\{Z(\mathbf{u})\cdot Z(\mathbf{u}+\mathbf{h})\right\}+E\left\{\left[Z(\mathbf{u}+\mathbf{h})\right]^2\right\} \end{aligned} \quad [1\text{-}1]$$

where Z is a random variable. This can be used to calculate the covariance between two points. The covariance between points separated by a distance **h** is:

$$C(\mathbf{h}) = E\{Z(\mathbf{u})\cdot Z(\mathbf{u}+\mathbf{h})\}-E\{Z(\mathbf{u})\}\cdot E\{Z(\mathbf{u}+\mathbf{h})\} \quad [1\text{-}2]$$

The variance (σ^2) is defined as the covariance at a distance **h**=0:

$$C(0)=\sigma^2=E\left\{\left[Z(\mathbf{u})\right]^2\right\}-E\{Z(\mathbf{u})\}^2 \quad [1\text{-}3]$$

Combining Equations 1, 2 and 3 under a decision of second order stationarity yields:

$$\gamma(h)=C(0)-C(\mathbf{h}) \quad [1\text{-}4]$$

In this way, the covariance between points separated by a distance can be calculated from the variogram. $\gamma(\mathbf{h})$ for multiple lag distances, $\mathbf{h}$, are often calculated from the available exploration data and then modeled with a positive definite function. The variogram model is most commonly used as an input parameter to estimate a variable in a domain using Kriging or to generate a series of realizations using SGS. Kriging is a linear estimator that assigns weights λ_i to the i^{th} data point $Z(\mathbf{u}_i)$ to estimate at a given location $\mathbf{u}$:

$$Z^*(\mathbf{u}) = \sum_{i=1}^{n} \lambda_i \cdot Z(\mathbf{u}_i) \qquad [1\text{-}5]$$

The weights generated by Kriging lead to an estimate that minimizes the error variance: the expected squared difference between the estimate at a location, $Z^*(\mathbf{u})$, and the true value at that location, $Z(\mathbf{u})$. This estimate has less variance than the original variable. This smoothness is well known and is addressed using SGS to add a random component to the Kriged estimate that corrects for the smoothing effect of Kriging. Kriging, SGS and the smoothing effect are well documented in literature, for example see Journel and Huijbregts (1978) and Deutsch (2002).

Variogram based techniques often assume the variable of interest follows a multi Gaussian distribution, which is fully defined by the covariances calculated from the variogram model. Often realistic results can be generated under a multi Gaussian framework using transformations; however, any parametric approach will be limited in that it cannot reproduce complex features unless they can be defined by the parameters, which is seldom the case. The limitations inherent in a multi Gaussian assumption are that the curvilinear features and ordering relationships present in geological formations cannot be reproduced, see Figure 1-2. Sequential indicator simulation (SIS) using the variogram from a TI is compared to a multiple point realization generated using SNESIM (Strebelle, 2002), see Section 1.1.4, and the same TI. Both simulations are conditioned to samples taken from the TI to attempt to reproduce the features of the TI, see Figure 1-1. The following indicator variogram was used in simulation:

$$\gamma(\mathbf{h}) = 0.015 + 0.145 sph_{\substack{ah1=24 \\ ah2=3.5}}(\mathbf{h}) + 0.0864 sph_{\substack{ah1=31 \\ ah2=18}}(\mathbf{h}) \qquad [1\text{-}6]$$

ah1 is in the 45 degree direction, *ah2* is in the 135 degree direction and *sph* is a spherical variogram structure defined by:

$$C \cdot sph\left(\frac{\mathbf{h}}{a}\right) = \begin{cases} C \cdot \left(1.5\frac{\mathbf{h}}{a} - 0.5\left(\frac{\mathbf{h}}{a}\right)^3\right), & if\ \mathbf{h} \le a \\ C, & if\ \mathbf{h} \ge a \end{cases} \qquad [1\text{-}7]$$

where C is the contribution given to the variogram structure and a is a range parameter which is defined for each principle direction.

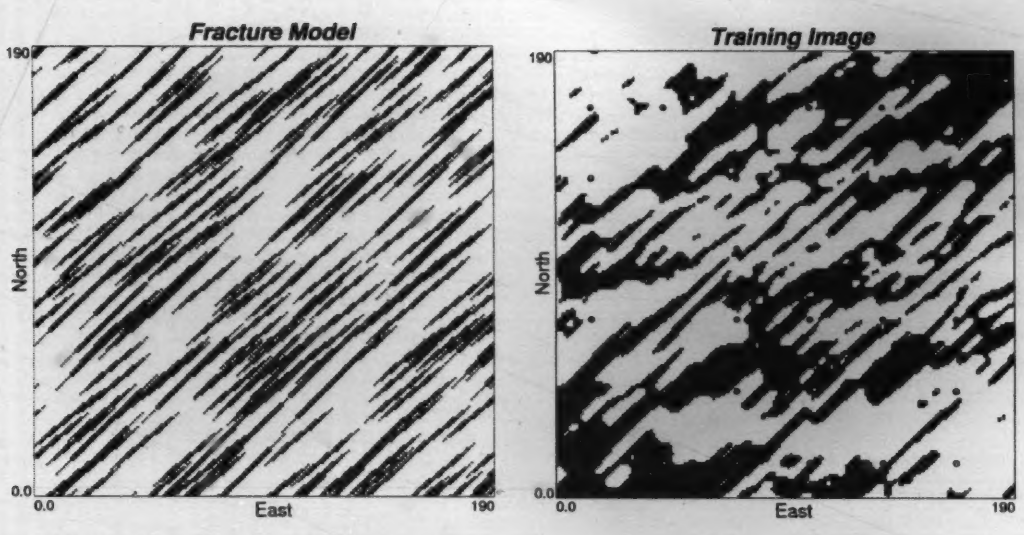

Figure 1-1: Fracture model (left) used to generate the TI (right). This TI is used in multiple point simulation, see Figure 1-2, and is used to generate the variogram for SIS, see Equation [1-6]. The TI is generated from the fracture model as per the methodology presented in Chapter 4. Scale for figures: a 190 by 190 grid with a unit block size.

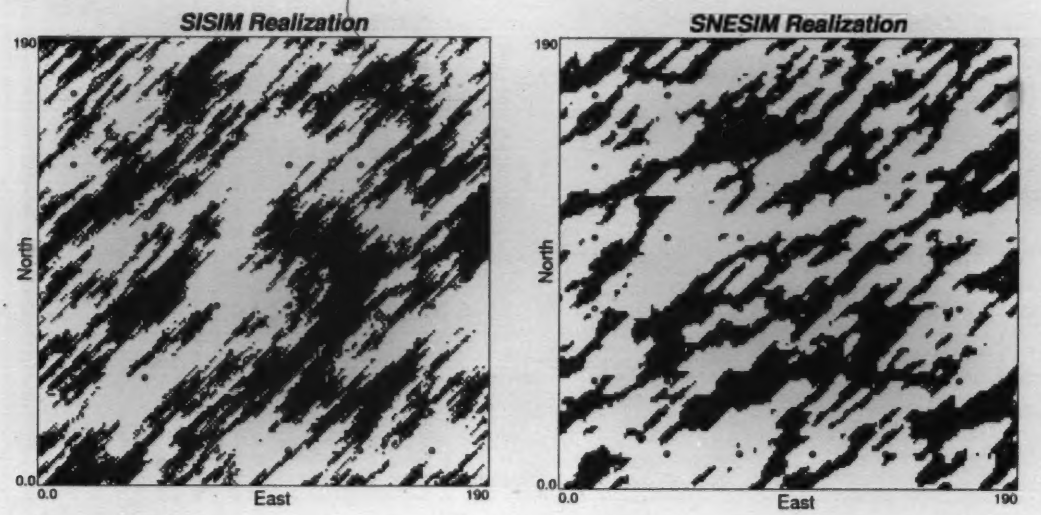

Figure 1-2: Left - A conditioned SIS using the variogram from the TI shown in Figure 1-1. Right– A multiple point simulation using the single normal equations (SNESIM) approach proposed by Strebelle (2002). Scale for figures: a 190 by 190 grid with a unit block size.

The curvilinear features that are obvious in the original TI are not reproduced with SISIM. The variogram is the only information that is taken from the TI and it can only capture the linear two point relationship. This is the limitation of using only the covariance between data points to generate realizations. For many applications,

reproducing the curvilinear features may be critical. The multiple point simulation in Figure 1-2 reproduces many of the complex features found in the TI and does not show the excess randomness characteristic of SIS. Ignoring these curvilinear features may have a significant effect on subsequent calculations such as reserves, grade, etc. The need to reproduce these nonlinear features in geostatistical realizations motivates the use of multiple point statistics.

1.1.3. Multiple Point Statistics

Multiple point statistics are any type of statistic that considers the relationship between more than one data point simultaneously. For this thesis, multiple point statistics are considered to be statistics that consider the relationship between more than two points (i.e. statistics beyond the variogram). Multiple point statistics are often compared to two point statistics and the difference will be made clear.

There are many different multiple point statistics such as: the connectivity function; the multiple point histogram; and the distribution of runs. The multiple point histogram and the distribution of runs will be used in Chapter 5 to select appropriate TIs.

The Distribution of Runs

Mood (1940) first derived the theoretical distribution of runs for a string of random numbers. Since then it has been used to test random number generators as the theoretical distribution of runs for a string of random numbers has an analytical solution. Runs will be calculated on drill holes and the distribution of runs will be used to match TIs to available exploration data. The concept is to count the number of consecutive occurrences of a particular category. This is illustrated in Figure 1-3.

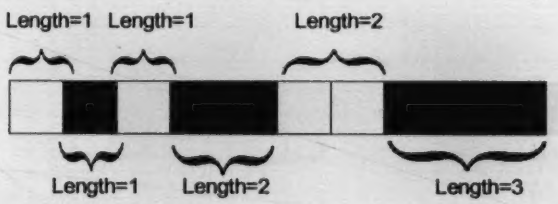

Figure 1-3: Example of calculating the distribution of runs for a drill hole represented here as a string of facies. These facies can be either white or gray and represent different rock types encountered in the drillhole at equally spaced intervals.

The distribution of runs for this example would be 3 runs of length one, 2 runs of length two, and 1 run of length three. The cumulative distribution of runs can be found by noting that each higher order run contains all lower order runs. For example, the run of three gray blocks contains two runs of length two and three runs of length one; therefore, the cumulative distribution would be: 10 runs of length one; 4 runs of length two; and 1 run of length three. Figure 1-4 shows the distribution of runs.

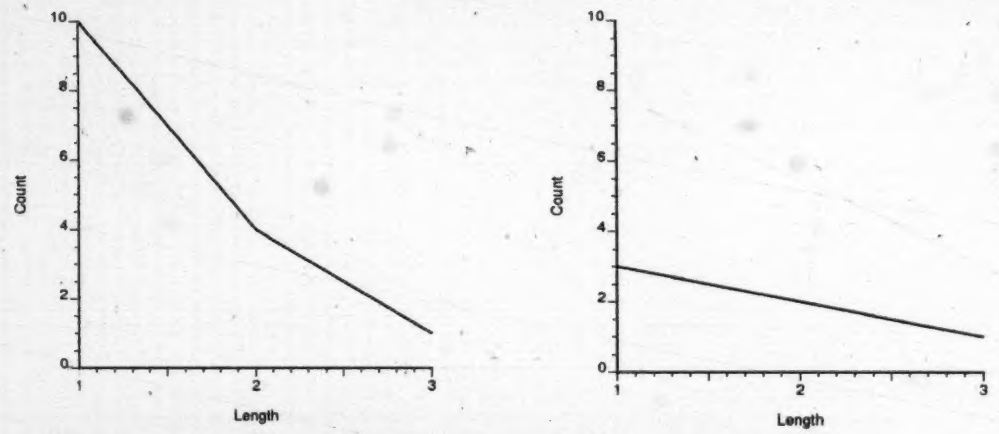

Figure 1-4: Left - cumulative distribution of runs. Right - distribution of runs.

It is not necessary that the spacing of the string of numbers be equidistant and parallel as depicted in Figure 1-3, but this simplifies the analysis. Runs are calculated on drill holes in Chapter 5 and it is practical to assume straight drill holes with equally spaced samples.

The Multiple Point Histogram

The traditional histogram counts the frequency of times a particular continuous variable falls in a bin or counts the frequency of times that a particular indicator variable occurs. The multiple point histogram counts the frequency of times a multiple point configuration occurs. Consider a 4 point configuration where each location can take two different categorical values, there are a total of 16 (2^4) unique configurations.

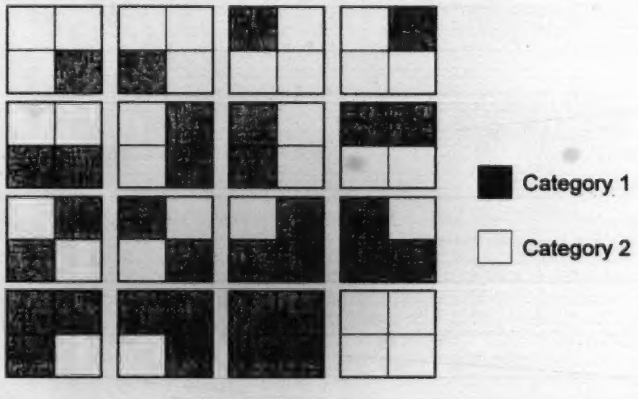

Figure 1-5: All possible arrangements of a 4 point configuration with two categories.

Considering this four point configuration or template, the multiple histogram for a gridded image can be calculated. The number of times that each configuration in Figure 1-5 occurs in the image is counted and the bins of the histogram correspond to the

different configurations. Consider the image in Figure 1-6 with the multiple point histogram shown in Figure 1-7.

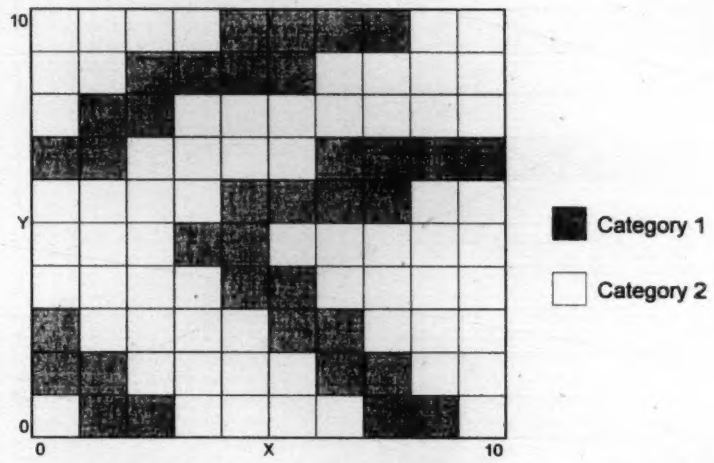

Figure 1-6: Example image to calculate the multiple point histogram. Figure scale: unit length, 10 by 10 blocks.

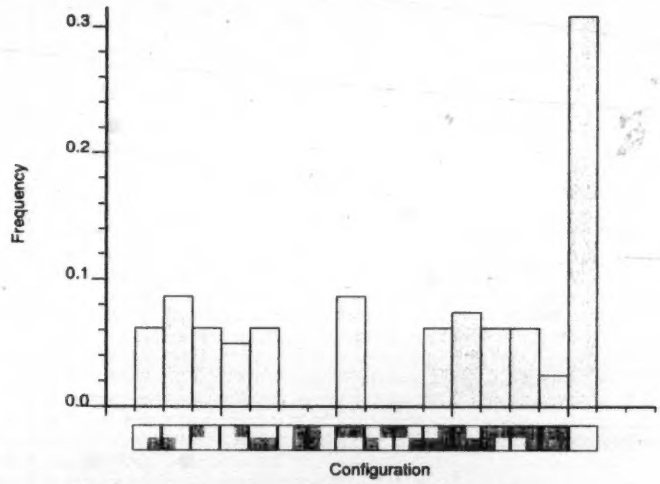

Figure 1-7: Multiple point histogram of the image in Figure 1-6.

Note that the ordering of the bins in Figure 1-7 is arbitrary. Considering a larger template or more categories significantly increases the number of bins in the multiple point histogram, which makes visualizing the multiple point histogram for large templates challenging. There is no limitation on the shape or size of the histogram other than the computational effort required to deal with the large number of bins. Other possible configurations are shown in Figure 1-8.

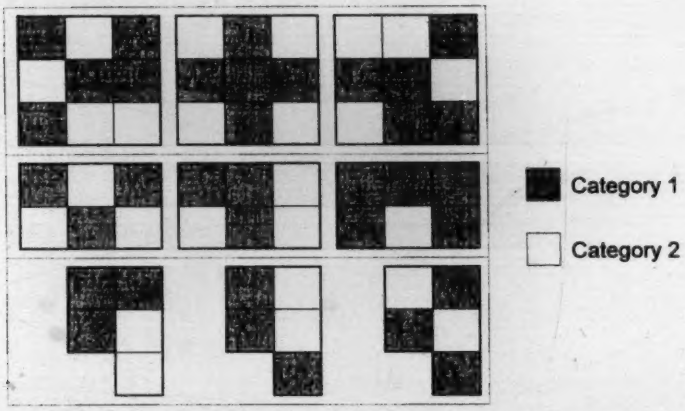

Figure 1-8: Three possible multiple point templates. Not all possible configurations are shown. Above – a nine point square template. Middle – a six point rectangular template. Below – a five point irregular template. Each block has a unit length.

1.1.4. Using Multiple Point Statistics

The multiple point histogram is commonly used in multiple point simulation algorithms. Traditionally, the variogram has been modeled based on exploration data. This is not possible when using the multiple point histogram because of the volume of data necessary to accurately infer all bins of the multiple point histogram. An alternative source for the inference of multiple point statistics is needed. Selecting a TI to be representative of the area of interest has become the most common method of inferring the necessary multiple point statistics.

Using multiple point statistics can be a difficult task. Consider that a 16 point statistic with 10 categories results in 10^{16} bins with each bin unrelated to adjacent bins. Having 10^{16} statistics makes inference difficult, thus it is common to select a TI that is representative of the deposit of interest to infer this large number of necessary multiple point statistics. It is also necessary that the TI is exhaustive and of sufficient size to ensure all statistics, such as the bins of the histogram, can be informed.

This thesis is targeted at generating the TIs necessary for inferring the multiple point statistics used in geostatistical simulation. Techniques available for multiple point simulation include: using the single normal equations (Guardiano and Srivastava, 1993 and Strebelle, 2002); using simulated annealing with the multiple point histogram as the objective function (Deutsch, 1992); updating conditional distributions with multiple point statistics (Ortiz and Deutsch, 2004); training neural networks for multiple point simulation (Caers, 2001); and using a Gibbs sampler (Lyster and Deutsch, 2006a). Refer to these sources for multiple point simulation techniques.

The most common multiple point simulation algorithm uses the single normal equations, SNESIM (Guardiano and Srivastava, 1993 and Strebelle, 2002). This method generates geostatistical simulations by applying Bayes' law, Equation [1-8], to calculate the conditional probabilities for each unknown location.

$$P(A|B) = \frac{P(A \cap B)}{P(B)} \qquad [1\text{-}8]$$

Consider the configuration of points in Figure 1-9. The unknown (?) location could be gray, white or black. The configuration of one gray category and two white categories can be found on the multiple point histogram and the conditional probabilities for the equations shown in Figure 1-9 are the frequencies of the multiple point histogram for the given configuration.

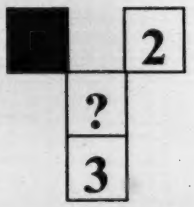

$$P(\text{White}) = \frac{P(? = \text{White}, 1 = \text{Grey}, 2 = \text{White}, 3 = \text{White})}{P(1 = \text{Grey}, 2 = \text{White}, 3 = \text{White})}$$

$$P(\text{Grey}) = \frac{P(? = \text{Grey}, 1 = \text{Grey}, 2 = \text{White}, 3 = \text{White})}{P(1 = \text{Grey}, 2 = \text{White}, 3 = \text{White})}$$

$$P(\text{Black}) = \frac{P(? = \text{Black}, 1 = \text{Grey}, 2 = \text{White}, 3 = \text{White})}{P(1 = \text{Grey}, 2 = \text{White}, 3 = \text{White})}$$

Figure 1-9: Inferring the conditional probabilities at an unknown location given three conditioning data at locations 1, 2 and 3. Each location is defined by a category: white, gray or black (no black categories are shown).

Simulation of the facies model proceeds by drawing a simulated value at the unknown (?) location based on the conditional distribution generated by Bayes' law and repeating for all unknown locations.

1.1.5. Vein Deposits

TIs will be developed for vein type deposits by mimicking vein formation; therefore, a conceptual understanding of the formation of veins is necessary. Specifically, the type of ore bearing fluid, its movement through fractured rock and the deposition of a mineral of interest from the fluid must be appreciated so that the expected structures can be mimicked.

The nature of the ore-bearing fluid will greatly affect the type of ore deposit formed. Each ore bearing fluid has its own unique properties: silicate-dominated magmas; water-dominated hydrothermal fluids; meteoric waters; seawater; connate waters; and fluids associated with metamorphic processes. Guilbert and Park (1996) describe the characteristics of these ore-bearing fluids in detail. This thesis is primarily focused on how these ore-bearing fluids move through their surrounding rock and deposit ore to form mineralized veins. To this end, the type of ore bearing fluid is only important insofar as it affects the viscosity and density of the fluid used in flow simulation.

The ore bearing fluid travels through the host rock obeying physical laws dictated by the fluids' viscosity and density, the host rocks' permeability, interconnected pores, fractures, faults and the natural pressure gradients due to insitu stresses (Guilbert and Park, 1996). Veins are created when the movement of these fluids is guided by major structures, such

as faults or fractures, and these fluids may even open new or closed fractures by hydrofracturing (Guilbert and Park, 1996).

Veins are created when the path of highest permeability through a rock is highly influenced by fracturing and faulting rather than by rock properties such as porosity and interconnected pore spaces. When this occurs, the fluid will preferentially flow though the faults and deposit minerals in vein type structures. Different types of faulting and folding are shown in Figure 1-10. Each type of faulting will result in a different type of vein structure.

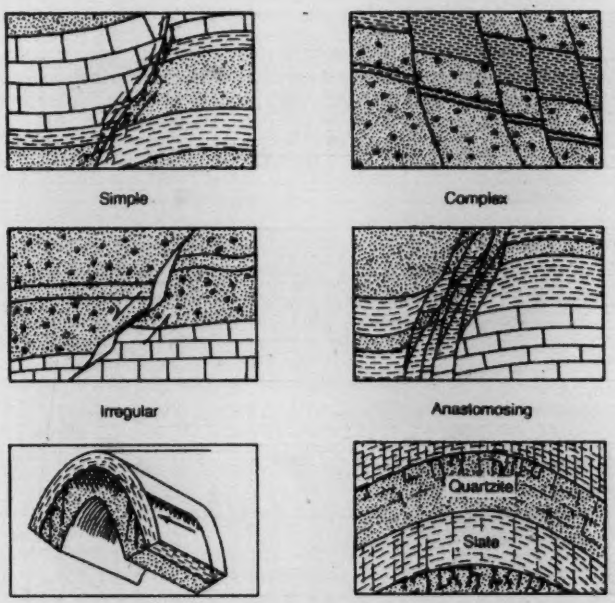

Figure 1-10: Types of basic folding and faulting (Guilbert and Park, 1996). Not to scale (NTS).

TIs for vein type deposits will be created by mimicking some of the natural processes that form veins. It is not necessary to reproduce all of the geological processes; rather, the goal is to generate TIs that have the correct geological features. This will be achieved while simplifying the formation process.

1.1.6. Weathered Deposits

TIs will also be created for weathered deposits such as laterites, saprolites, and bauxites. The following discussion will give a brief overview of the processes that create the boundary between the weathered and non-weathered rock. Typical profiles for these types of deposits are presented to provide the necessary background to evaluate the geologic realism of the proposed TIs.

The overall process of weathering is the combined effect of physical, chemical and biological processes on a parent rock. The outcome of weathering can be to: erode away a potentially economic ore body; leach away a valuable mineral, reducing the economic

worth of the deposit; concentrate a valuable mineral, increase economic worth; or chemically alter the mineralogical makeup of the ore deposit (Guilbert and Park, 1996).

The chemical portion of weathering occurs because the original rock, formed under high temperature and pressure, is not in equilibrium when exposed to the low temperature, low pressure, high humidity and variable pH of the surface. As water from the surface flows through these newly exposed rocks, the potentially low pH surface water containing trace carbon dioxide chemically alters the rock. The processes involved in chemical weathering include hydration, solution, oxidation, reduction, hydrolysis and chelation, see Bland and Rolls (1998) for a detailed description of these processes.

Physical weathering is considered to be weathering that occurs without changing the chemical composition of the rock. This can take the form of dissolving, crystallization, freeze thaw cycles, etc, see Bland and Rolls (1998) for a complete list and description. Physical weathering often occurs in tandem with chemical weathering, as the chemical weathering process often weakens the integrity of the rock and thereby make physical weathering more effective.

Biological weathering is thought to be secondary to physical and chemical weathering (Guilbert and Park, 1996; Bland and Rolls, 1998) and is not critical to the understanding of the formation of the boundary between the weathered and non-weathered layers in an ore deposit. Therefore, the reader is referred to Bland and Rolls (1998) for a description of biological weathering.

When the combination of physical, chemical and biological weathering erode, dissolve and transport a mineral of interest such that the subsequent deposition increases the concentration of the mineral, the process is called supergene enrichment. If the concentration is increased sufficiently, a weathered type ore deposit is created. Supergene enrichment most commonly occurs with iron, aluminum, copper, and manganese (Guilbert and Park, 1996) because of the chemical and physical properties of these minerals. These weathered deposits have a distinctive bedded profile consisting of a soil layer followed by layer of highly weathered rock, a layer of weathered rock and underlain by the original parent rock, see Figure 1-11. These layers form because of the interaction of the water percolating through the rock and its behavior once reaching the water table at the time of weathering. Each subsequent layer, moving downward in the horizon, is defined by a marked decrease in the degree of weathering from the completely weathered soil to the intact host rock. The naming of the layers in the profile vary in literature. Hereafter, the highly weathered layer will be deemed laterite and the less weathered layer saprolite (after Bardossy and Aleva, 1990). The boundary between the soil and laterite, as well as between the laterite and saprolite is continuous; however, the transition occurs over a scale of centimeters up to a few meters (Bardossy and Aleva, 1990). For mining purposes this boundary will be considered a sharp contact between layers and will be modeled as such.

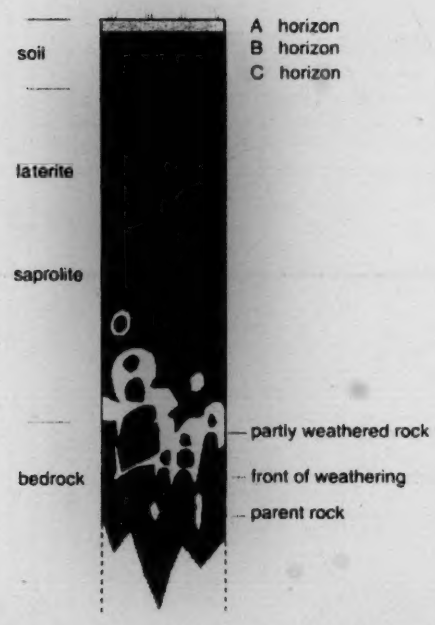

Figure 1-11: Typical horizon of a weathered deposit. Modified from Delvigne (1998). NTS.

Bardossy and Aleva (1990) describe the contact between weathered layers as an "irregularly shaped, downward attacking interface, with broad, retarded embayments and deeply penetrating and advancing tongues." (pg. 48). What they mean by this description is shown by the irregular nature of the contact between the laterite and the saprolite in Figure 1-11, specifically, the jagged nature of the contact and the pockets of material that appear. These are the types of features that will be important to reproduce in a TI.

Figure 1-11 is an idealized view of a weathered contact. The exact nature of this boundary will vary by deposit. To obtain a better idea of some of the typical features seen in weathered boundaries, Figure 1-12 and Figure 1-13 show geological interpretations of weathered contacts and Figure 1-14 shows a photograph of a weathered contact. Note the irregular nature of the boundary and the presence of boulders in both the geological interpretations and photographs.

In the case of generating TIs for weathered deposits the formation process will not be mimicked. The goal of TI generation is to generate facies models that reproduce the features of the deposit. The formation processes of a weathered deposit are presented so that the features of the TIs generated can be compared to the features of actual weathered deposits. TIs for weathered deposits will be created using SGS to generate the desired nonlinear features, such as the downward attacking interface and boulders, described in this section.

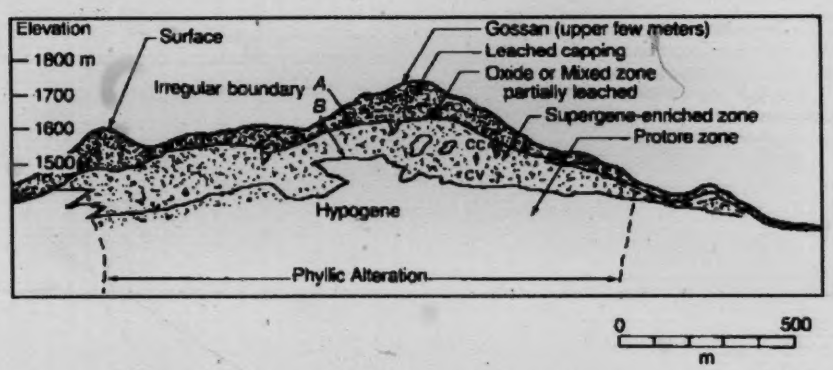

Figure 1-12: Geological interpretation of a gold/copper laterite profile at La Caridad, Sonora, Mexico (modified from Guilbert and Park, 1996). Scale shown on figure.

Figure 1-13: Geological interpretation of a laterite profile near Poços de Caldas, Brazil (modified from Bardossy and Aleva, 1990). Scale shown on figure.

Figure 1-14: Photograph of an iron bauxite contact on a mined bench (modified from Bardossy and Aleva, 1990). White outline added to highlight the irregular nature of the weathered contact. Unknown scale.

Chapter 2: Data for Training Images

The most geologically realistic source for the inference of multiple point statistics is extensively sampled deposits or reservoirs. Reliable blasthole or production data that cover the area of interest is only available after extraction. However, production data from a similar deposit could be used to infer the necessary statistics rather than use a TI. Exhaustive data that may be available prior to production include blasthole data from a mined out deposit that is similar to the deposit of interest or production data from a similar area.

Some examples of data sets that could be used as TI are presented, followed by published examples of simulated data that could be used in place of actual data. Simulated data can take the form of geostatistical simulations, scanned images or geological interpretations.

2.1. Data Sets as TIs

Using data or models generated from exhaustively sampled areas ensures the TIs are geologically realistic. Presented below are data sets that could be used as TIs for geologically similar deposits. Associated statistics are included to aid in TI selection.

2.1.1. Anglo American Data

Anglo American has extensively drilled a gold vein deposit in South Africa. This data set, provided by Anglo American, would only be appropriate for a similar deposit in that area, but if the deposit of interest shows similar features to this deposit, this exhaustive dataset could be used as a TI. Figure 2-1 shows maps of the available variables: facies; thickness of the vein; and thickness x grade. Note that gold grade can be determined by dividing thickness x grade by the thickness. The reef of interest, the Ventersdorp Contact Reeft, is a near horizontal conglomerate bed that contains the gold. Figure 2-1 shows a projection of the available drillhole data onto a horizontal plane with the thickness of the reef providing the third dimension of the deposit. Histograms for all variables are shown to help determine if this dataset is appropriate for a given area of interest, see Figure 2-2.

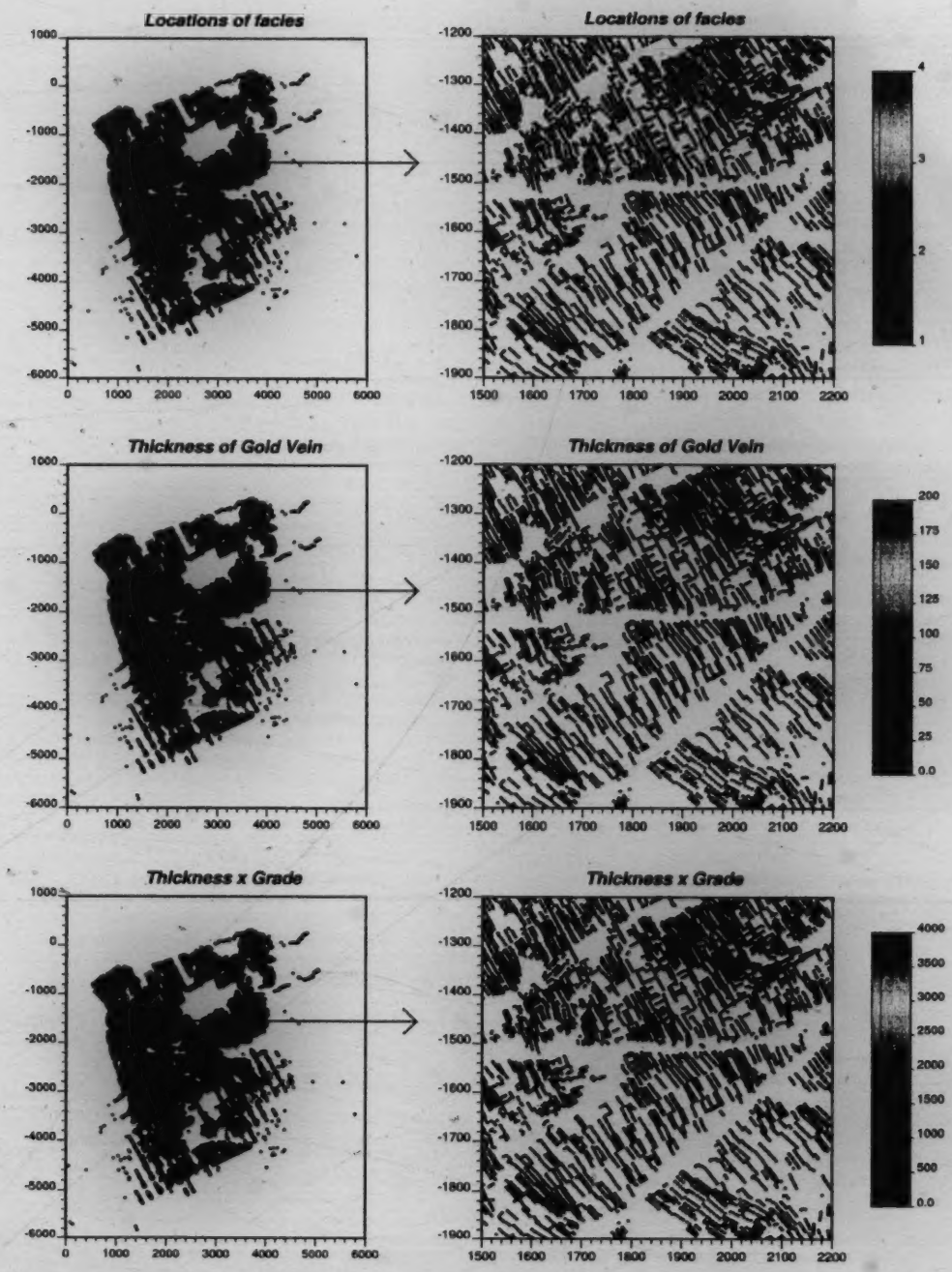

Figure 2-1: Maps showing the location of the samples in the Anglo American dataset. Maps on the right show a close up of the highlighted area. Units of the map are km, thickness in cm, and grade in g/t. The vertical axis is north and the horizontal axis is east.

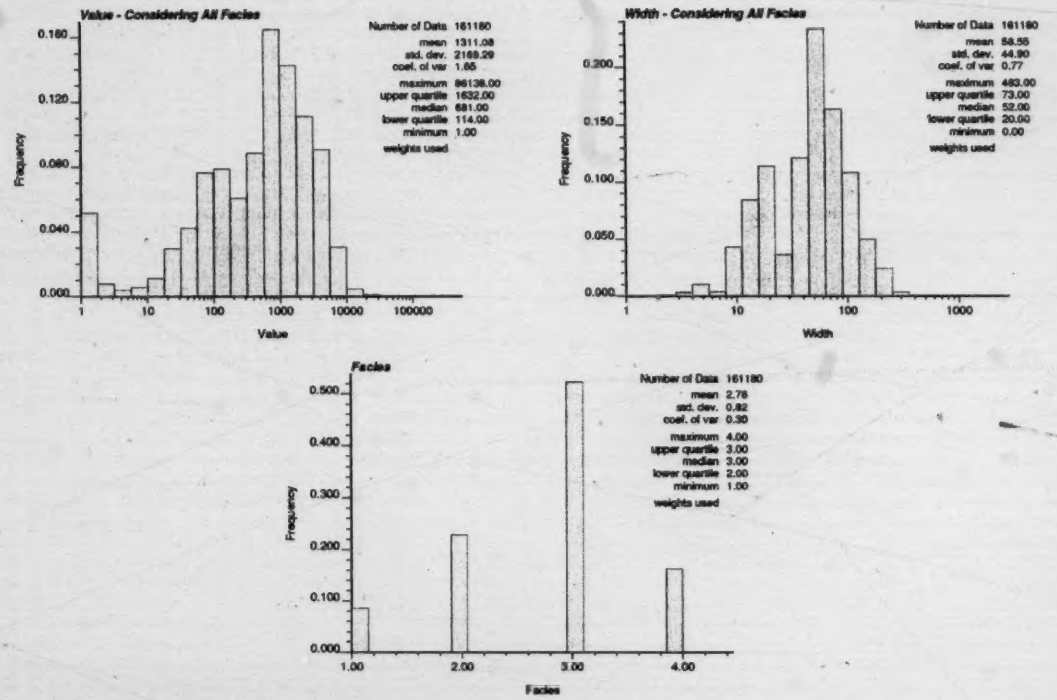

Figure 2-2: Histograms for the Anglo American dataset.

There is a very high density of samples in this area. A total of 161180 samples cover an area of about 10km^2, resulting in an average spacing of 8m. This densely sampled gold vein would be appropriate for an area showing similar features.

2.1.2. Walker Lake Data

The Walker Lake data set has been used extensively for demonstrating geostatistical concepts. The two dimensional data set contains two variables, U and V, which are functions of an extensive digital mapping of elevation from Walker Lake, Nevada. Both variables relate to the roughness of the terrain. The Walker Lake data set is an extensively sampled area and could be used as a TI for variables showing similar characteristics. It would be most appropriate for an elevation type variable, as the majority of the roughness is based on elevation detail. More details on the origins and specifics of the data can be obtained from Isaaks and Srivastava (1989) and the data set can be obtained from http://www.ai-geostats.org/resources/data/WalkerLake.zip. Figure 2-3 shows maps of the variables and Figure 2-4 shows the histograms and scatter plots for the two variables.

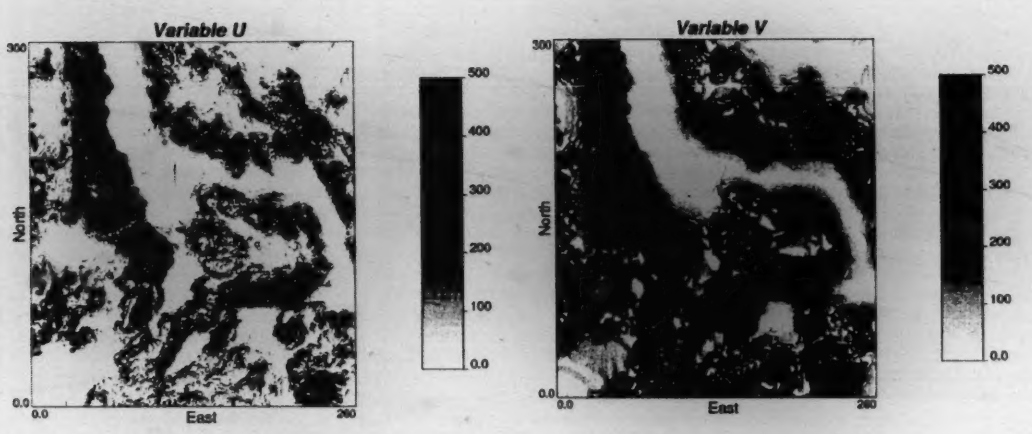

Figure 2-3: Maps of the Walker Lake variables. Blocks are unit size.

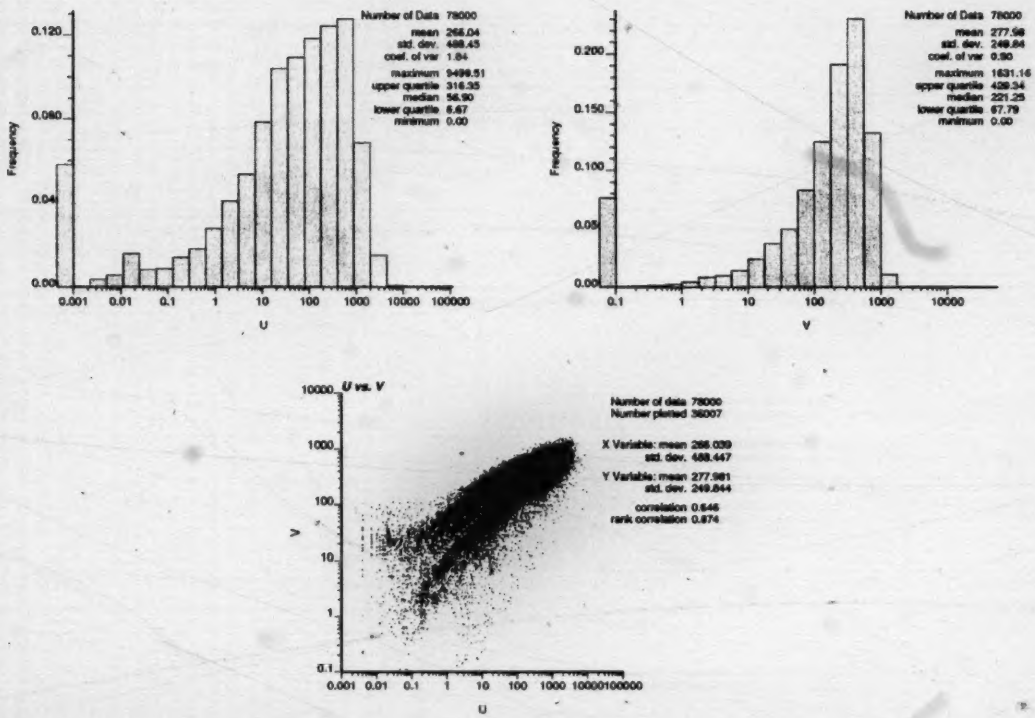

Figure 2-4: Histograms and scatter plot of U and V variables for the Walker Lake data set.

2.1.3. Discussion

Using a data set as a TI should be done with care as many problems hinder the use of exhaustive data for multiple point statistical inference:

- Lack of flexibility – There is very little opportunity to adjust the data to fit the area of interest. Properties such as anisotropy, geological units, complex geometry or proportions of the extensively sampled area must be representative of the area of interest and are difficult to alter to fit new areas. For example, if the production data are available for a vein type deposit, but the vein thickness is slightly larger, it would be difficult to adjust this and use the data as a TI.
- Lack of availability – It is rare that one company will develop two areas that are sufficiently similar to use data from the older area to infer multiple point statistics; this, coupled with companies reluctance to share data in its original form, makes obtaining extensively sampled data difficult.
- Lack of gridded data – Even when production data are available it is seldom on a regular grid. Current multiple point simulation algorithms are limited to using TIs that are defined on a regular grid because of the difficulty in defining a multiple point template for an unstructured grid. Production data must be altered to fit a regular grid and this can pose problems. Alternatively, dense production data could be used to generate a very detailed and accurate geostatistical model on a regular grid.

Selecting a data set as a TI when it does not contain the exact geological characteristic of the variable being modeled will impose the incorrect structure on the facies model. One solution is to use simulated data or object based modeling to generate a TI with the desired structure. This allows the modeler more flexibility when selecting an appropriate TI.

2.2. Simulated Data

TIs can also be generated by simulating geological processes. This has been done by Pyrcz and Deutsch (2003), Pyrcz et al. (2005) and Pyrcz and Strebelle (2006) for fluvial and deepwater TIs. Mimicking geological processes is also the basis for the TIs presented in Chapter 3 for vein type deposits. Moreover, scanned images can also be used as simulated data for TIs; an example of this follows.

2.2.1. Training Image Library

The difficulties in using production data for TIs has resulted in the use of process based modeling to generate TIs that have realistic geological features, such as the training image library presented by Pyrcz and Deutsch (2003) for fluvial and deepwater TIs. Mimicking geological processes generates TIs that are exhaustive and contain the desired geological features. The fluvial TIs are generated using FLUVSIM (Deutsch and Tran, 2002) to create channels which are modified based on the bank retreat model to be more geologically realistic. The deepwater TIs are based on a surface based model of

compensational cycles of flow events within turbidite lobes. In total, there are 294 TIs that are 256x256x128 blocks and have various net to gross ratios and geological features. Cross sections of some of the TIs are shown in Figure 2-5 and Figure 2-6.

2.2.2. Scanned Images

There are numerous freely available photographs, outcrop maps, geological interpretations and sketches of deposits and reservoirs. It is possible to use these scanned images to generate TIs. Using these types of images provides thousands of geologically realistic 2-D TIs. Figure 2-7 shows a scanned image of a sedimentary rock that could be used to capture the bedded nature of certain mineral deposits.

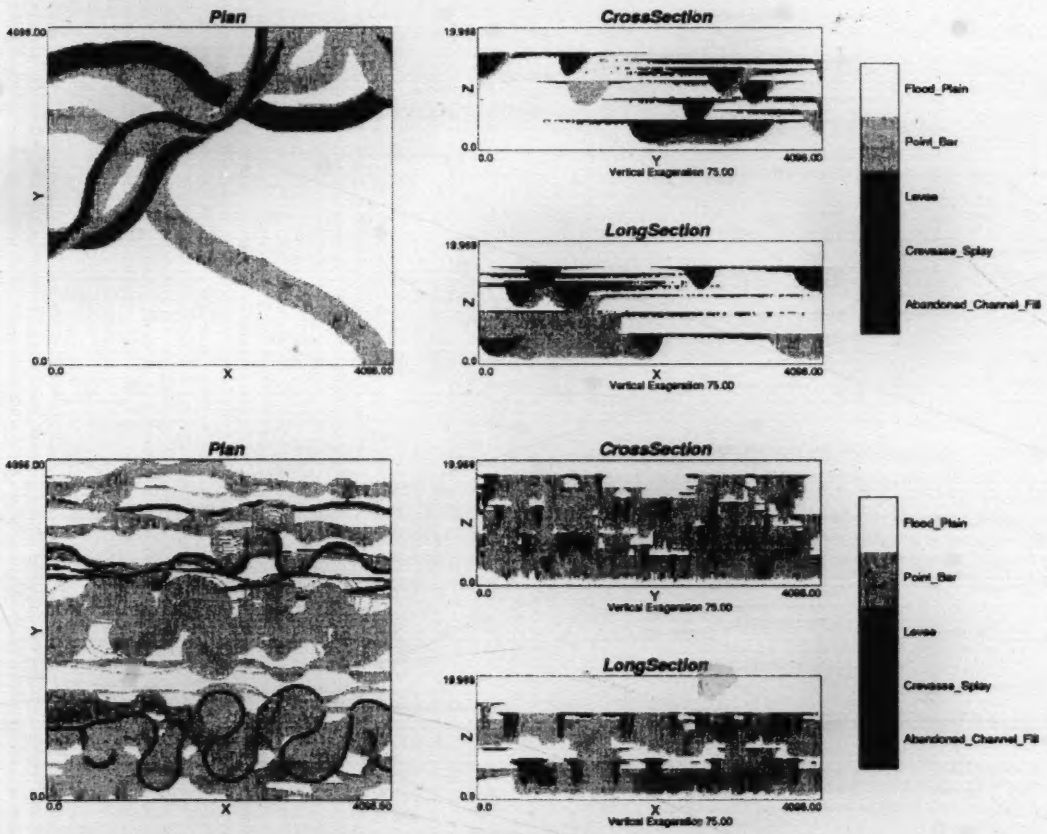

Figure 2-5: Example fluvial TIs from Pyrcz and Deutsch (2003). Above – Net to gross of 0.2, channels 100 units wide and median sized lobes. Below – Net to gross ratio of 0.6, channels 20 units wide and small sized lobes. Unit block size with dimensions shown on figures.

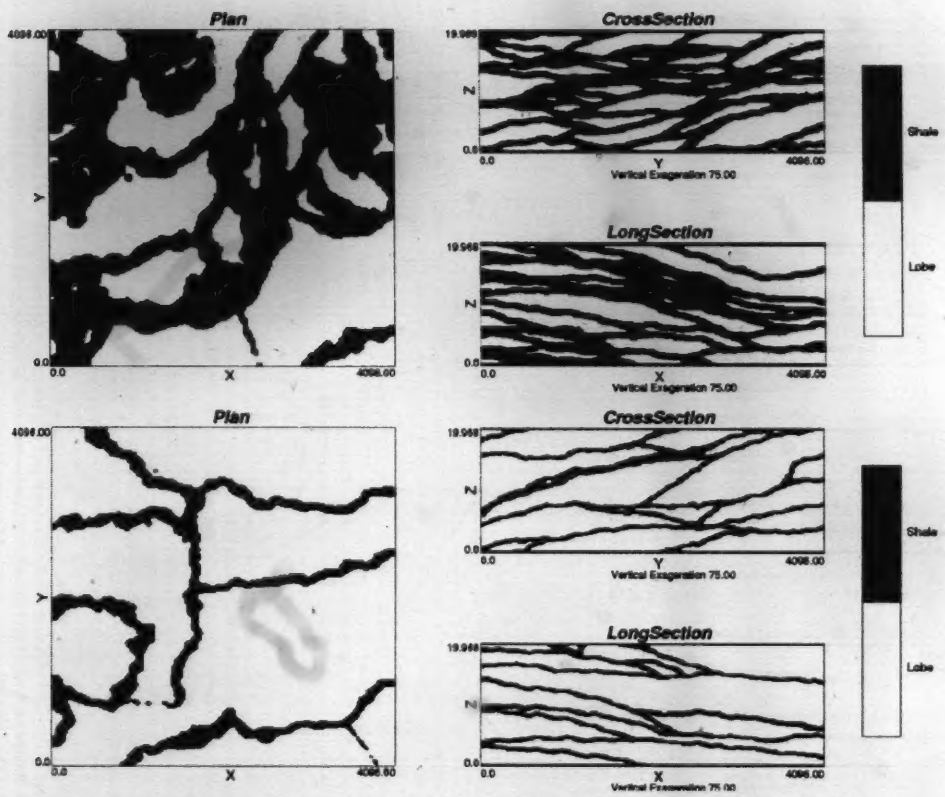

Figure 2-6: Example deepwater TIs from Pyrcz and Deutsch (2003). Above – Net to gross of 0.4 and median sized lobes. Below – Net to gross ratio of 0.8 and large sized lobes. Unit block size with dimensions shown on figures.

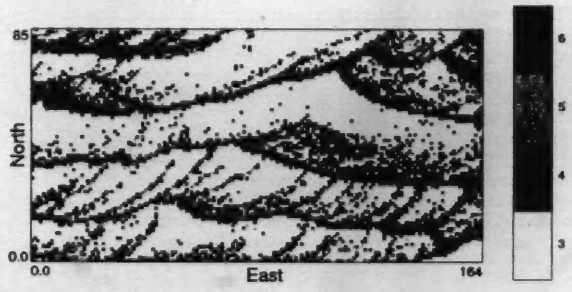

Figure 2-7: Example of a scanned image that could be used as a TI for a bedded type deposit. Unit block size with dimensions shown on figure. Facies definitions based on color of scanned rock.

Chapter 3: Process Based Vein Type Training Images

The difficulties discussed concerning using data as a TI leads naturally to creating an algorithm that can generate realistic TIs that is adaptable to site specific conditions. TIs will be created by mimicking the formation of veins. The basis for the proposed methodology depends on the availability of a fracture model, which can be created in several ways. Stochastic simulation (Chilès, 1989) and available physical models (Takayasu, 1985) are two possible sources of fracture models. The following methodology will focus on a fracture model created for the Whiteshell area in Ontario, Canada, as provided by Srivastava (2002). The following TI generation methodology could be applied to any fracture model to reproduce site specific vein properties such as direction of strike, thickness, length, shape etc.

3.1. Proposed Methodology

In order to generate a realistic TI, the movement of the ore bearing fluid through the fractured host rock will be modeled by applying a flow simulation to a fracture model. The TIs will be created by associating areas of high flow with vein locations. Specifically, the methodology for generating TIs for vein deposits consists of the following steps, explained in greater detail below:

1. Generating a fracture model;
2. Modeling the permeability of all areas in the model;
3. Running a flow simulation on the permeability model; and
4. Creating a TI by considering veins to be areas of high flow.

One idea would be to use the fracture models directly as a TI, bypassing many of the steps in the proposed methodology; however, there are a number of undesirable features present in fracture models that make it desirable to use them as input to flow modeling first. Figure 3-1 shows a section of Srivastava's (2002) fracture model for the Whiteshell area. The fracture model is a highly detailed model based on a variety of data sources; see Srivastava (2002) for further details on the fracture modeling methodology.

The fractures are disjointed and end abruptly making Figure 3-1 inappropriate for use when modeling vein deposits. This is the motivation for using flow simulation through the fracture model, as desirable features such as connectivity can be controlled. The resulting TIs appear to be more realistic.

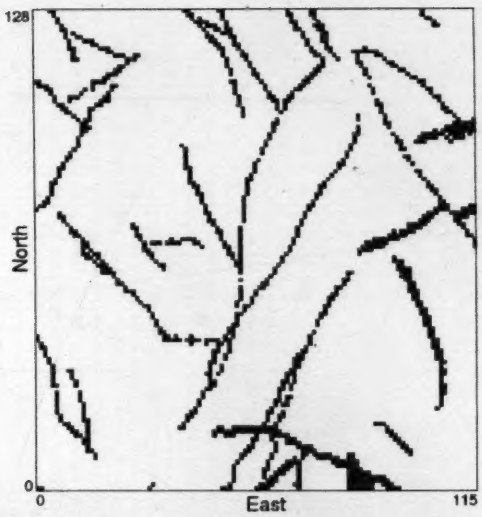

Figure 3-1: Typical horizontal slice of the Whiteshell fracture model. Originally the fractures are planar features described by triangular facets but have been rasterized into a block model. Unit block size.

Much research has been done in the area of fracture modeling, for example see Rossmanith (1998) or Faybishenko et al. (2000) and NRC (1996). Reviews of past work on flow through fractured media can be found in Sahimi (1993) and Lee and Farmer (1993). More recent work done in the field can be found in NRC (1996), Alsop et al. (2004), and Faybishenko et al. (2000).

3.1.1. Step 1: Fracture Model Generation

Fracture models can be obtained from: (1) programs that seed fractures and then propagate them according to known stress regimes; (2) programs that draw fracture characteristics from a distribution and place these objects randomly in a model; or (3) from models of areas where the fractures and faults have been extensively mapped.

The fracture model is extremely important for the generation of a TI as it has a large influence on the features present in the final TI. The following should be considered when generating the initial fracture model:

- Fracture spacing – This will influence the density of veins in the TI.
- Sets of fractures – If there are multiple sets of veins in the deposit, fractures corresponding to all directions should be created.
- Fracture orientation – This will control the direction(s) of anisotropy.
- Fracture terminations – A high density of fractures could result in instances when a newer fracture will be truncated by an older fracture. This would affect the overall flow regime of the model.

- Fracture shape – The exact shape of a fracture differs with fracture type (braided, regular, irregular, complex, conjugate, etc). Moreover, fractures often flatten with depth (Srivastava, 2002).

A realistic TI depends on the choice of an appropriate fracture model and should consider the features mentioned above. The fracture model of a specific deposit must be inferred from site-specific observations and other similar deposits. Types of information that will be available during exploration that will help infer the fracture model include: fracture mapping of outcrops; fractures encountered in exploration holes; orientation of fractures in nearby mined areas; inference of stress regimes in the area; and expert geological interpretations.

3.1.2. Step 2: Permeability

In order to run a finite difference flow simulation on a fracture model, the permeability of the area must be established. Unlike permeability modeling in the petroleum industry, which commonly depends on a stochastic approach conditioned to available well logs, core plugs and/or seismic data, this particular application requires a permeability model in the absence of conditioning data. The resulting TI will be used to create geologic features for the purpose of constructing heterogeneous models of mineral grades.

In the example presented below, see Section 3.2, it is assumed that the area of interest is characterized by a binary mixture of fractured and non-fractured rock at an arbitrary grid resolution. The permeability of the fractures is uniform, but higher than the permeability of the surrounding host rock. Refinement of the TI and a sensitivity analysis of the resulting images to different permeability values are considered in a later section.

3.1.3. Step 3: Flow Rate Calculation

A steady state flow simulation is then run on the permeability model to calculate the pressures in each block. The flow simulator used in the example is FLOWSIM (Deutsch, 1987), which applies a constant pressure gradient across the model in one direction with no flow boundary conditions on the other faces in the model, as shown in Figure 3-2.

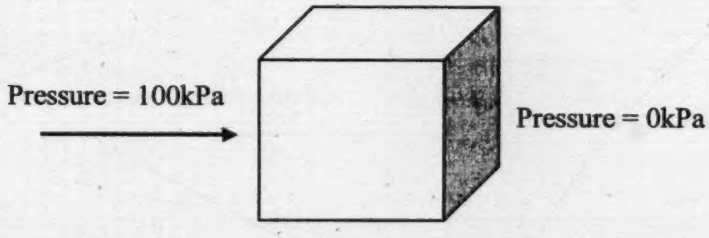

Figure 3-2: Pressure gradient in the x-direction with the box representing the 3D fracture model.

This flow simulation generates the pressure in each block of the fracture model. From the pressure difference between blocks, the flow into and out of each block can be calculated from Darcy's law:

$$Q = \frac{-kA}{\mu}\frac{\Delta p}{L} \qquad [3\text{-}1]$$

where Q is the volumetric flow rate, A is the surface area of the face through which flow occurs, k is permeability, Δp is the change in pressure across the volume, L is the length of flow, μ is the fluids viscosity. In this case water is used as the ore bearing fluid. In this version of Darcy's law the change in elevation is ignored.

The calculation of the total flow rate through a single block in the model is shown in Figure 3-3 for a two dimensional case. The net flow rate in a block will be zero because of the conservation of mass; therefore, the absolute flow rate from each block into (or out of) the block is summed to obtain the flow through the block. This will calculate a flow rate that is actually twice the flow rate in the block, but the relative magnitudes of twice the flow rate will still give an accurate picture of where the veins are located, so this Q is used.

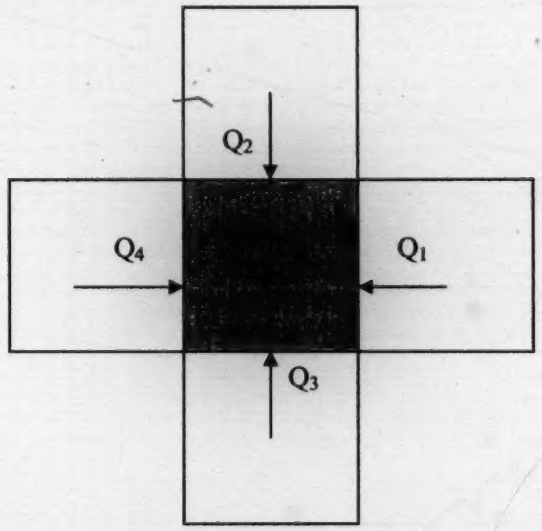

$$Q = |Q_1| + |Q_2| + |Q_3| + |Q_4|$$

Figure 3-3: Calculation of the total flow rate in a single block (gray block) in a 2D model.

Since FLOWSIM only considers flow in the direction of the pressure gradient, multiple flow simulations considering flow in all three principal directions should be considered. The absolute flow rate for a block is calculated for each pressure gradient (see Figure 3-4) and the sum of the three flow rates is taken as the total flow rate through the block.

This is not the actual flow rate in the block, but a high value for this flow rate will correspond to a high flow rate for the ore bearing fluid.

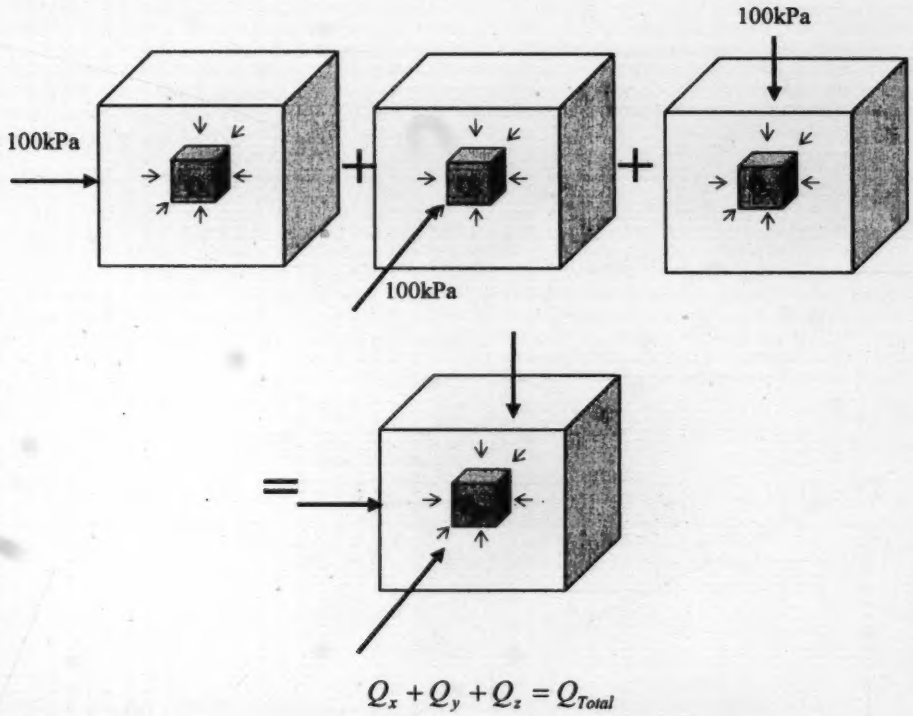

Figure 3-4: Calculation of the total flow rate in a block for three pressure gradients.

3.1.4. Step 4: Locate Veins

The final step is to apply a threshold cutoff to the flow rates. Veins are identified by blocks that have a high flow rate. This is analogous to locating areas that had a high flow of ore bearing fluid at the time of vein formation. The threshold on flow can be adjusted depending on the desired vein structure. The highest flow rates are located in the blocks that contain fractures with the flow rate gradually decreasing in nearby blocks. Narrow veins can be generated by applying a relatively high threshold on the flow rate. If this threshold is decreased, additional blocks will fall above the threshold, thus generating a thicker vein structure.

3.2. Example

The proposed methodology is applied to a section of Srivastava's (2002) fracture model of the Whiteshell area in Ontario. This highly detailed fracture model was created to model the flow of contaminates around a nuclear dump site. Figure 3-5 is an image of the fault model. To illustrate the methodology, only a small area (approximately 10%) of

this fault model is used to generate TIs. This smaller area consists of over 150,000 blocks (specifically, 115x128x11); Figure 3-1 shows the orientation of the faults in this area for a specific aerial slice of the 3D model. This horizontal slice will be used throughout this paper to examine the effects of changing different parameters in the process to generate different TIs. All TIs are generated in 3D.

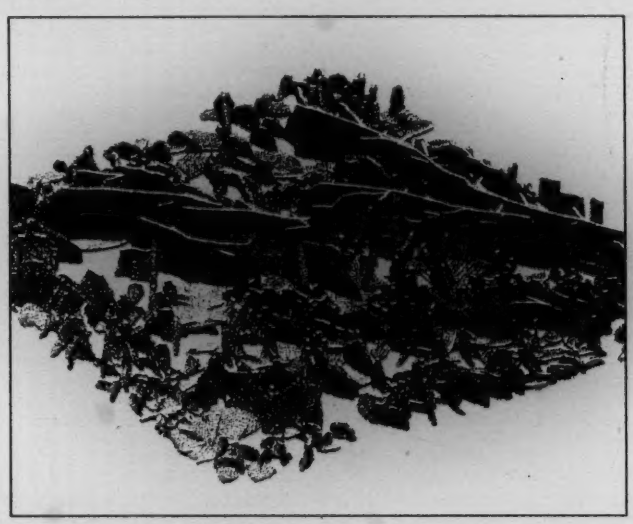

Figure 3-5: View of the fracture model. Fractures are shown in gray, the host rock is transparent. NTS but the area covered is 12km by 12km.

3.2.1. Steps 1 and 2 – Fracture Model and Permeability

The fracture models used for this paper were generated by Srivastava (2002) by merging geostatistical techniques with fracture modeling principles. This fracture model is a discrete fracture model where each fracture is defined by a triangular mesh or surface. For the purposes of flow simulation, a block model of permeability is created from the discrete model; blocks containing a fault are assigned a high permeability and areas without faulting are assigned a low permeability. The exact permeability values are varied in order to assess the effect of permeability on the final TI. For the example that follows an aspect ration of 10:1 will be used; the faults will be assigned a permeability of 10 while the host rock will have a permeability of 1.

3.2.2. Step 3 – Flow Rate Calculation

A flow simulation of the permeability model is run using FLOWSIM (Deutsch, 1987) and the pressure in each block is obtained. Pressure gradients in the x and y directions are considered. Figure 3-6 is a slice showing the pressure in each block and is typical of all pressure slices in the model. When the pressure gradient is in the y direction the result is visually identical but rotated. As described previously, the pressure in each block is used with Darcy's law to calculate the absolute value of the flow rate in each block for each pressure gradient.

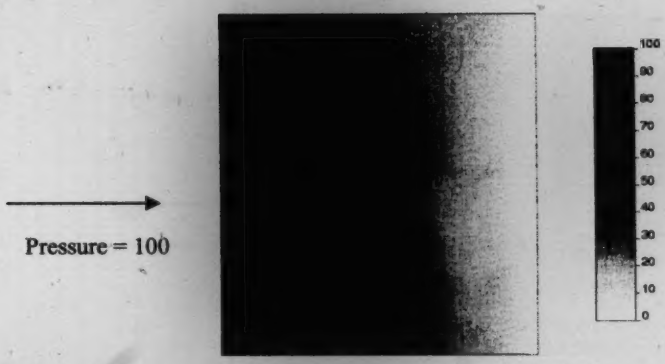

Figure 3-6: Typical slice of pressure with a horizontal pressure gradient generated from FLOWSIM (Deutsch, 1987). Pressure is shown in kPa.

The flow rate for both the *x* and *y* direction pressure gradients are shown in Figure 3-7 with the pressure gradients indicated. Two areas where the effect of changing the gradient direction is most noticeable are highlighted. Moreover, notice that there are many anomalies near the boundaries of the faults. Often low flow rates are seen on the fault boundaries; this is not desirable as there should be high flow near the faults and low flow between faults. Figure 3-8 shows the effect of combining the flow rates in the x and y directions.

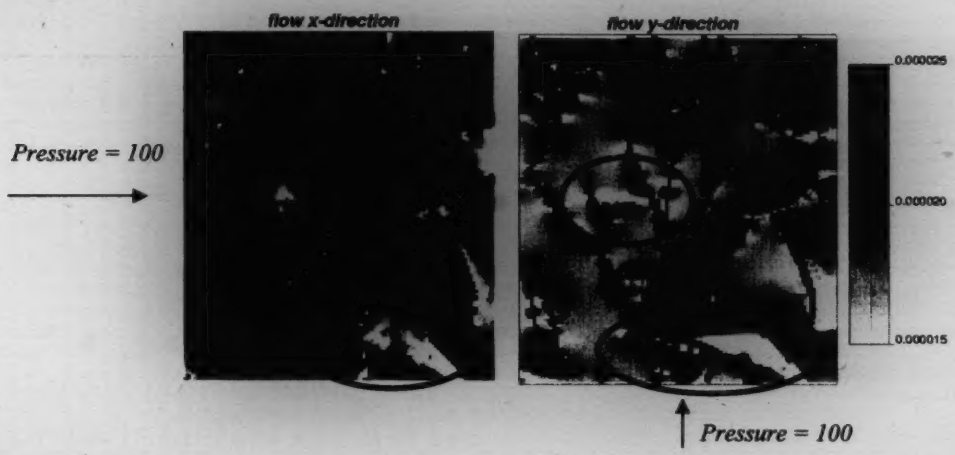

Figure 3-7: Total flow in the model for pressure gradients in the x and y directions. Aspect ratio is 10:1.

Figure 3-8: Combined flow in the model for pressure gradients in the x and y directions.

Many of the anomalies near the fault boundaries in Figure 3-7 are not as prevalent in Figure 3-8 because the flow rates in the two directions are combined. The areas of low flow are still present in Figure 3-8, but the flow rates are more continuous at the boundaries between high and low flow rates. This boundary effect may be further mitigated by also considering the flow rate in the *z* direction.

3.2.3. Step 4 - Locate Veins

The images in Table 3-1 show how different aspect ratios for the permeability affect the final TI. The aspect ratio is defined as the value of the permeability for the blocks containing a fracture divided by the permeability of the blocks without a fracture. For example, an aspect ratio of 2:1 assigns fractured areas a permeability of 2 while the host rock receives a permeability of 1. Different thresholds on total flow rates are also applied to generate multiple TIs. Decreasing the threshold assigns more blocks to be mineralized and has the effect of allowing the vein to expand further into the surrounding rock. In this way, thicker veins can be created. Moreover, a cleaning algorithm, maximum a posteriori selection (MAPS) (Deutsch 1998), could be used on each TI to smooth out rough areas and create a more continuous TI. MAPS uses a moving window average and applies weights to each nearby block depending on the distance from the block in the center of the moving window, see Deutsch (1998) for a detailed explanation of the MAPS algorithm.

Table 3-1: Horizontal sections of the final TIs showing the effect the aspect ratio and threshold have on the TIs. Images have been cleaned with MAPS (Deutsch 1998). Black represents the locations of the veins and white represents the location of the rock matrix.

	Aspect Ratio = 3:1	Aspect Ratio = 10:1
Low Threshold on Flow Rate	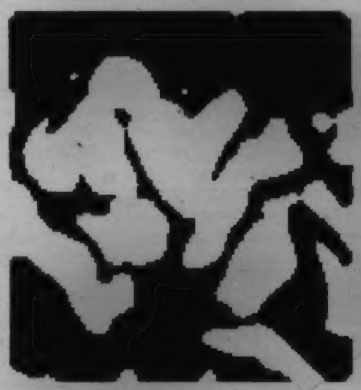	
Medium Threshold on Flow Rate	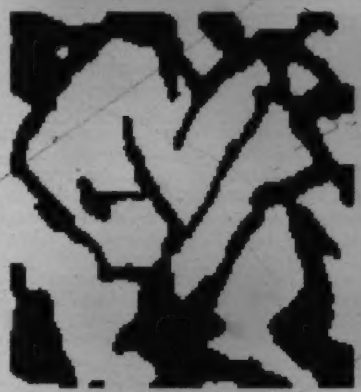	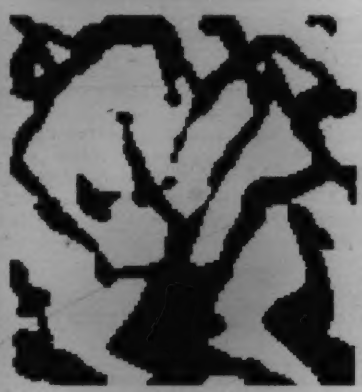
High Threshold on Flow Rate		

3.2.4. Discussion

The distance the vein extends into the rock matrix can be controlled using either the aspect ratio or the threshold cutoff; increasing the aspect ratio or the cutoff will restrict the veins' expansion into the rock matrix. This allows the user to create different TIs based on the geology of the veins being modeled.

In general, the TIs seem to connect unconnected faults in a logical manner. The faults in the fracture model are connected to nearby faults using the path of least resistance. Some locations where this occurs are highlighted in Figure 3-9.

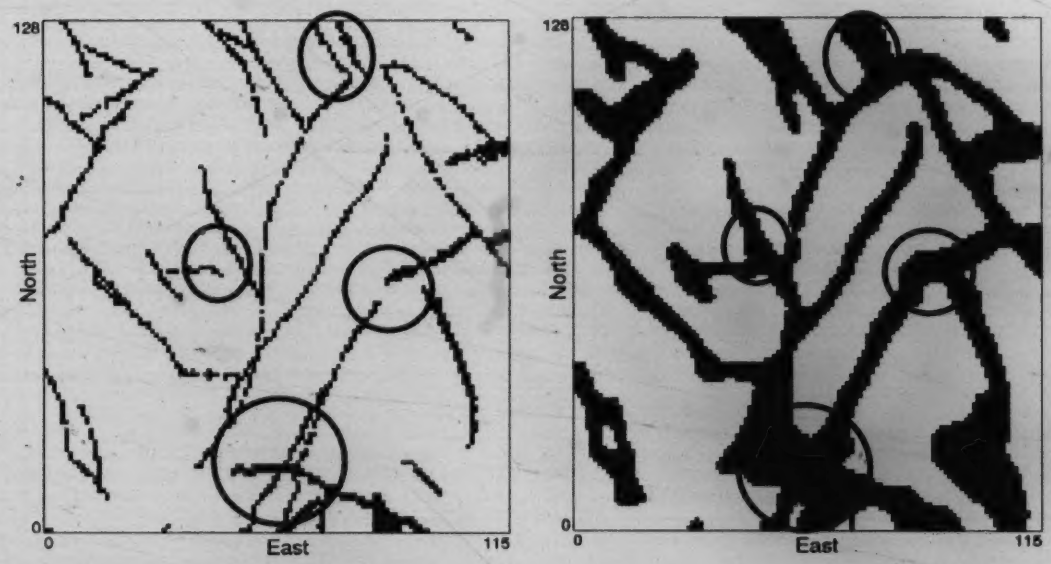

Figure 3-9: Left – Initial fault model; Right – TI with a 10:1 aspect ratio and a high flow cutoff. Highlighted areas show locations where the disconnected faults have been realistically connected to form a continuous vein structure.

As mentioned previously, the disjointed nature of the fracture model is not seen in the TI generated using a flow simulation thus, making the TI appear more realistic. To better assess the realism of these images they are compared to geological interpretations of actual vein deposits. Figure 3-10 compares the TI with a geological interpretation of a gold mine in Nova Scotia. The circled regions show areas of similarity. Both images show thickening of the veins in areas where there are high degrees of fracturing, as well as braided characteristics. There is more braiding in the gold mine cross section, but it can be seen that some of this braiding occurs in the TI and a change in the fracture model could control the level of braiding seen in the TI.

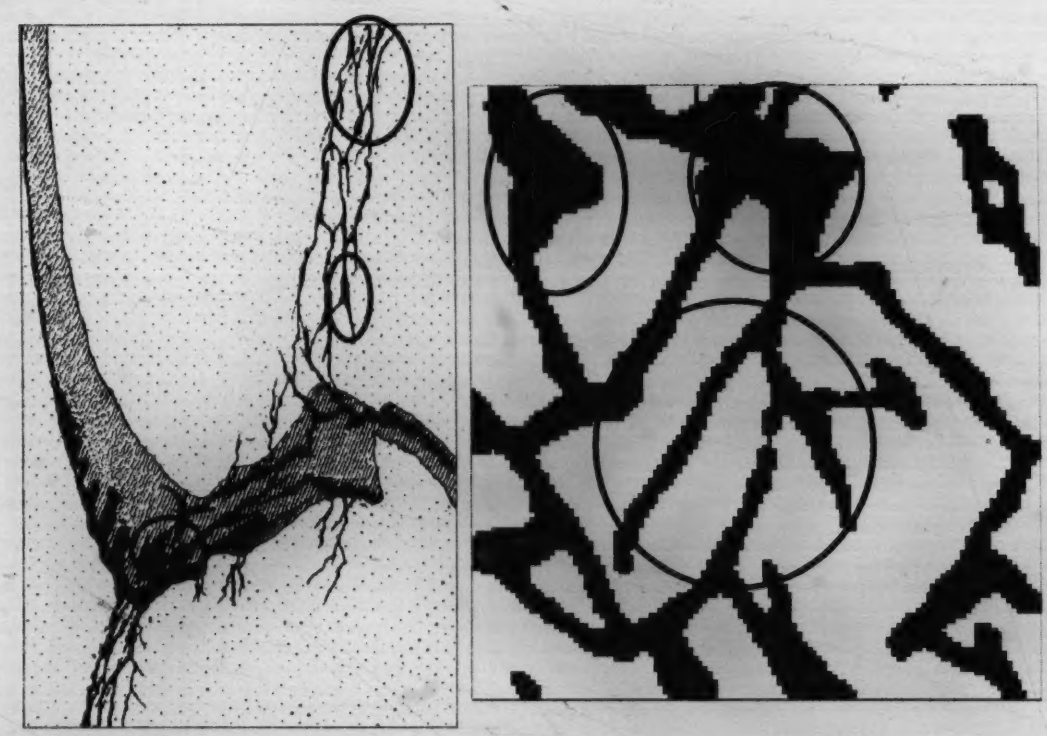

Figure 3-10: Left–West Lake gold mine, Mount Uniacke, Nova Scotia (as cited in Guilbert and Park, 1996), unknown scale. Right – Rotated TI with a 10:1 aspect ratio and a high cutoff. Highlights – braiding and thickening.

Similar features can also be seen in the TI and the Louvicourt Goldfield deposit shown in Figure 3-11. The thickenings are very similar, as are the areas that show some pockets of rock surrounded by veins. Braiding is also evident in both images as was seen before in Figure 3-10.

Figure 3-11: Left–Louvicourt Goldfield deposit at Val d'Or in Quebec (Robert and Poulsen, 2001), unknown scale. Right–Rotated TI with a 10:1 aspect ratio and a high cutoff. Highlights–rock pockets surrounded by veins and thickening of the veins.

In comparison with actual vein deposits, the TIs generated using Srivastava's (2002) fracture model seems to reproduce some features. Important characteristics such as braiding and thickening of the veins seem to mimic what is seen in the two gold deposits. Further manipulation of the fracture model would likely result in increased similarity between the TI and the gold deposit interpretations.

It should be highlighted that the criteria for validating these TIs are subjective, since the TIs will be considered as a good model of the facies of the deposit if they are similar to the interpretation the geologist generates based on expert knowledge and the information gathered through several sampling and logging campaigns. The actual geological architecture may differ from this interpretation and so will the TIs.

TIs can be conditioned to hard and soft data subsequently using a multiple point simulation method, providing a model for the geology that can account for the uncertainty of the interpretation. TIs should be considered only if they make sense from a geological viewpoint. The methodology proposed aims at providing a way to transfer the geological knowledge into a numerical model.

Chapter 4: Weathered Deposit Training Images

Weathered deposits are often characterized by boundaries between layers that display different degrees of weathering (Bardossy and Aleva, 1990). These boundaries are an important feature to model and will be simulated with sequential Gaussian simulation. The resulting realizations can be used as TIs that contain the non-linear characteristics of the boundary between weathered layers.

4.1. Proposed Methodology

Realistic TIs will be created by modeling the boundary between two weathered zones. The important geological features to reproduce include: 1) the erratic nature of this boundary as seen by the sharp changes in the boundary direction, often bypassing some material to weather deeper material and 2) the pockets of laterite material that appear in the saprolite zone and the pockets of saprolite that appear in the laterite zone, see Chapter 1. The boundary modeling will be accomplished by using SGS to simulate the laterite and saprolite zones. Specifically, the methodology for generating TIs for weathered boundaries consists of the following steps, as explained in greater detail below:

1. Generating synthetic drill hole data for the depth of the weathered contact (or use actual drill hole data if available)
2. Assigning a positive value to the laterite zone and a negative value to the saprolite zone
3. Performing SGS with the drill holes
4. Appling a threshold of 0 to the realizations generated in step 3 to define the laterite and saprolite zones; and
5. Using MAPS to smooth the contact and remove unwarranted randomness generated by simulation

4.1.1. Step 1: Synthetic Drill Hole Data for Control Points

An initial depth for the boundary between the laterite and saprolite layers below the topography is created by simulating a depth to contact variable on a coarse grid. Figure 4-1 shows an idealized initial grid and depth to the boundary.

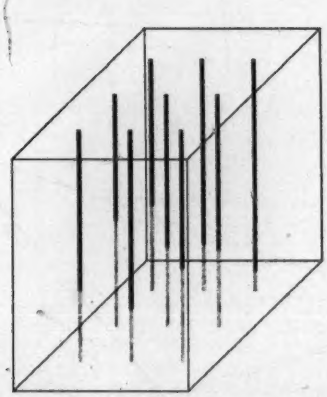

Figure 4-1: Coarse grid for simulation of the initial depth of the boundary. Dark gray – laterite. Light gray– saprolite. NTS.

These drill holes will be considered the control points for the weathered boundary. The drill holes are created by simulating a 2-D normal scored variable with SGS. The variable represents the depth to the boundary at each drill hole location. This depth variable is scaled so that each depth is positive and has the desired range. For example, multiplying the normal score variable by 5 and adding a mean depth of 15 will generate a contact that will have an average depth of 15 units and will cover approximately ±10 units. Changing these factors will change the depth over which the contact varies and can be used as a tuning parameter for generating a TI with the desired structure. Actual drill holes for a deposit of interest could be used as the control points to generate a site specific TI.

4.1.2. Step 2: Assigning Conditioning Data for SGS

The depth of the contact has been defined by the simulation described above. The drill hole will be populated in such a way as to generate a realistic boundary. Features of a realistic contact include: maintaining a certain minimum depth below the surface as it may be unrealistic to have outcrops of fresh rock; encouraging small scale irregularities; and, boulders occurring with greatest frequency near the boundary. To reproduce these features the drill holes will be populated with values near 0 at the contact and will have increasingly negative values to the bottom of the drill hole and increasingly positive values to the top of the drill hole, see Figure 4-2. Once simulated, the boundary will be defined as the zero contact in the model. Arranging the drill hole values in this way will force the boundary to pass through the control points at 0 but also allow it to fluctuate between drill holes, generating irregularities in the boundary and the pockets.

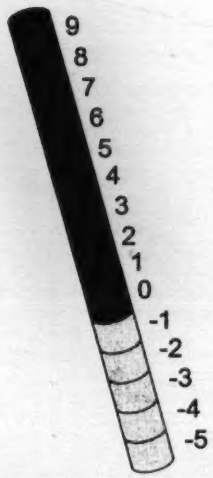

Figure 4-2: Example drill hole showing how the positive and negative values are assigned. Dark gray– laterite. Light gray– saprolite. NTS.

In addition to adding control points in the form of pseudo-drill holes, the location of the boundary on the edges of the model can be fixed. This can be done by adding conditioning data around the model as a skin, see Figure 4-3. All edge values of the model can be assigned positive and negative values, this will have two main effects: 1) the boundary will be forced to a user defined depth along the edges of the TI and 2) the high positive and negative values at the top and bottom of the model will tend to reduce the irregularities seen in the boundary.

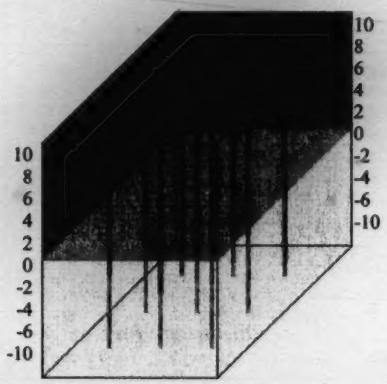

Figure 4-3: A skin of positive (dark gray) and negative (light gray) conditioning data can be added to the edges to control the boundary. NTS.

The skin shown in Figure 4-3 would constrain the boundary at the edges of the TI. This may be undesirable. Thus an alternative would be to include the skin on the top and bottom portions only. This would have the effect of limiting the irregularities in the boundary without constraining the edges, see Figure 4-4.

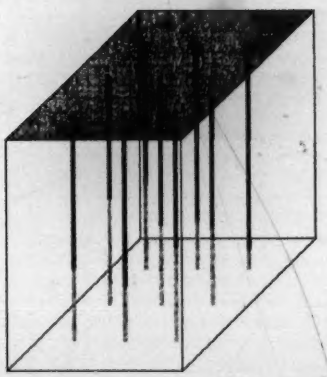

Figure 4-4: A skin of positive (dark gray) and negative (light gray) conditioning data can be added to the top and bottom to control the boundary without constraining it at the edges. NTS.

The magnitude of the positive and negative values added to the skin will affect the irregularities seen in the boundary. When higher values are added to the top and bottom of the model the boundary will tend to be pushed to the center for the model and will be relatively flat.

An important implementation detail when using the skin around the drill holes has to do with the timing of when the data is normal scored for SGS. If a skin is used, a constant value should be applied to the top and bottom edges of the model. The drill holes should be normal scored and then the skin can be added as conditioning data in normal units. The resulting distribution will not be normal but the goal of this simulation is not to reproduce a given distribution but to generate a realistic TI and hence a perfectly normal distribution is not needed for SGS.

4.1.3. Step 3: SGS

SGS will be used to populate the model with positive and negative values. Conditioning data for this simulation could take various forms, as described in Section 4.1.2, including:

- Drill hole data only
- Drill hole data and a skin on the top and bottom of the model
- Drill hole data and a skin around the entire model

Two important considerations when performing SGS are the choice of variogram and the search for conditioning data. Both of these will have a large effect on the look of the TI. A variogram with a longer range will tend to flatten the boundary and reduce the number of pockets. Moreover, using a larger search or more conditioning data from the search will have a similar effect. The effect of the variogram, search, and conditioning data options on the resulting TI can be found in Section 4.3.

Finally, a threshold of 0 will be applied to the simulations to generate the 3-D TI. Each image will be binary, with values >0 defining the upper oxidized layer and values <0 defining the lower less-oxidized layer.

4.1.4. Step 4: Smoothing

Even with a nugget effect of zero, the random nature of SGS will lead to realizations with too much short scale variability to be realistic. An idealized boundary between weathered layers is often depicted as smoother than an SGS realization would show (see Chapter 1 for figures of weathered contacts). Actual deposits may show characteristics that are more similar to the noisy realizations generated by SGS, see Figure 4-8. However, MAPS (Deutsch, 1998) can be used to smooth the realization and create a boundary that is similar to an idealized weathered contact. Either the SGS realization or the MAPS (Deutsch, 1998) smoothed model could be used as a TI for multiple point simulation depending on site specific conditions.

4.2. Example

The proposed methodology is applied with an 80x80x30 block model to demonstrate the process. Images of a larger model follow the example.

4.2.1. Steps 1 and 2: Synthetic Drill Hole Data

Using SGSIM (publicly available in the standard GSLIB package, see www.gslib.com), an unconditional SGS was performed on a coarse grid to simulate the depth to the boundary for use as control points. Sixteen drill holes are generated 20 units apart with an average depth of 14, see Figure 4-5. Simulation was performed with the following variogram, see Chapter 1 for a definition of the *sph* variogram structure:

$$\gamma(\mathbf{h}) = 0.2 + 0.8 sph_{\substack{ah1=50 \\ ah2=50 \\ vert=30}}(\mathbf{h}) \qquad [4\text{-}1]$$

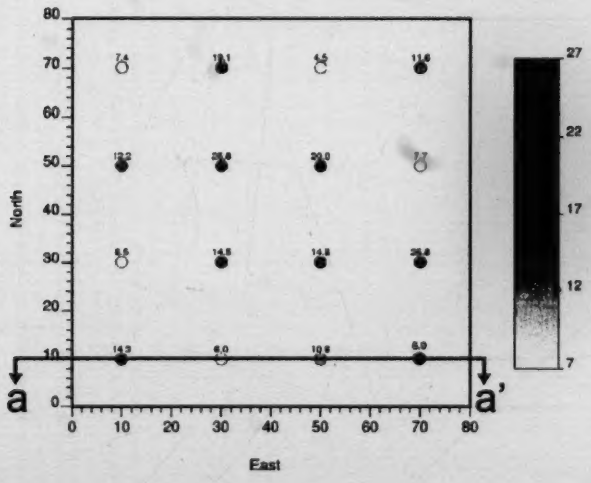

Figure 4-5: Drill holes showing the initial control points for the depth to the boundary. Scale represents unit depth to the contact at each location. Section aa' can be found in Figure 4-6. Drill holes spacing is 20 units.

The drill holes are then populated by assigning positive and negative values increasing away from the depth to the boundary. A cross section for the first row of drill holes located at y=10 is shown in Figure 4-6.

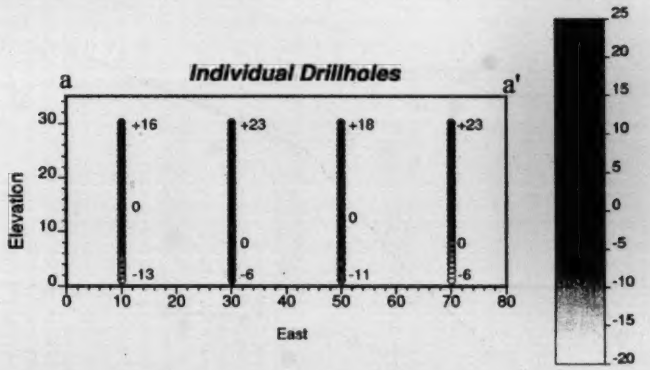

Figure 4-6: Section aa' - drill holes assigned positive and negative values, increasing away from the boundary. Minimum, maximum and the boundary (zero value) are shown for each drill hole. Drill holes spacing is 20 units.

The location of the zero values in these drill holes is determined by the control points shown in Figure 4-5. No skin will be added to this example. The effect of adding a skin can be found in Section 4.3.

4.2.2. Steps 3: SGS

The boundary must be created in three dimensions between all drill holes. This is done by simulating with the above drill holes and a zero nugget effect. The lack of a nugget effect will ensure the 0 boundary is continuous. The parameters in simulation will control how erratic the boundary is and how many pockets appear, see Section 4.3. Simulation with the following arbitrary variogram is shown in Figure 4-7, see Chapter 1 for a definition of the *sph* variogram structure.

$$\gamma(\mathbf{h}) = 1.0 sph_{\substack{ah1=30 \\ ah2=30 \\ vert=10}}(\mathbf{h}) \qquad [4\text{-}2]$$

The ranges selected for the variogram to be used in simulation should be considered relative to the spacing of the pseudo drill holes. In this example, the range is about 3/2 the spacing of the control points. A range shorter than the distance between control points will create a boundary that is more erratic. Finally, a threshold is applied to obtain the boundary between the laterite and the saprolite layers, see Figure 4-8.

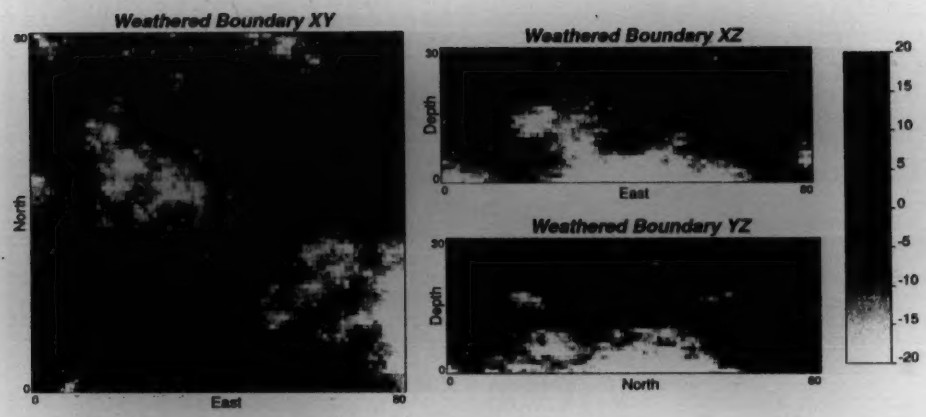

Figure 4-7: Simulated positive and negative values of the distance function. Each block has unit width.

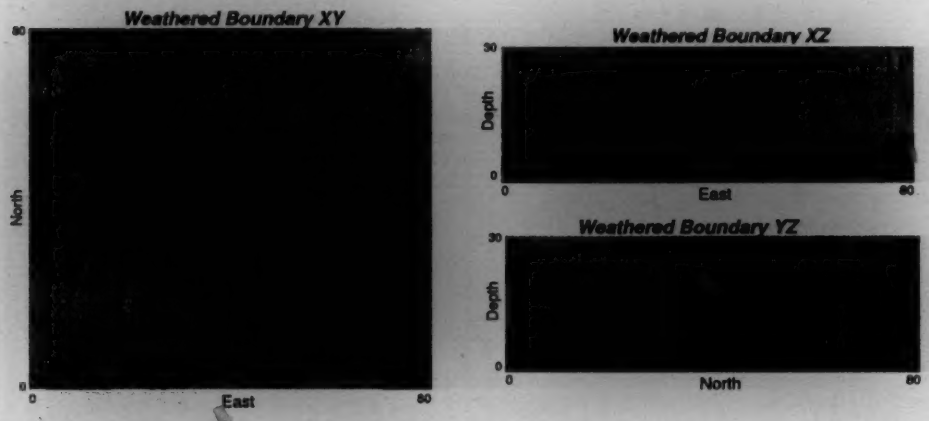

Figure 4-8: Simulated values with a threshold of 0 applied to define the boundary. Light gray– laterite. Dark gray – saprolite. Each block has unit width.

4.2.3. Step 5: MAPS Smoothing

The use of simulation to define the laterite and saprolite rock types introduces excessive randomness and may require smoothing. MAPS (Deutsch, 1998) is used to define a smooth boundary and only retain pockets of significant size, see Figure 4-9.

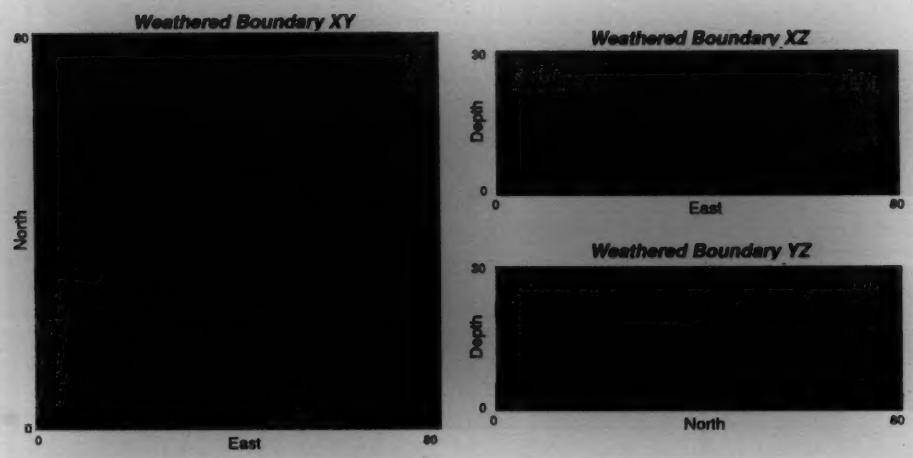

Figure 4-9: Smoothed using MAPS. Light gray – laterite. Dark gray – saprolite. Each block has unit width.

4.3. Sensitivity

There are a number of parameters in this methodology that can be used to generate boundaries with different characteristics. These parameters include:

- Control Points – the number of control points used in the domain will control the global shape of the boundary. The number of control points must be considered relative to the number of blocks in the model, and the variogram/search parameters of SGS must be considered relative to the spacing of the control points.
- Conditioning data options – drill holes are used as control points for the boundary. In addition to this, conditioning data can be added to the edge of the model to flatten the boundary or to constrain it to a user defined depth near the edges of the TI.
- Variogram parameters – the range/anisotropy of the variogram used when simulating the distance function will either increase or decrease the erratic nature of the boundary. It is necessary that no nugget effect be used to keep the contact continuous.
- MAPS smoothing – the degree of smoothing will control the level of randomness in the final TI.

Showing TIs for different values of all of the above parameters would result in many images. Therefore, Table 4-1 will summarize the effect of all parameters and a few examples are shown in Figure 4-10, Figure 4-11, and Figure 4-12.

Table 4-1: Sensitivity of weathered TIs to input parameters.

Parameter	Effect on Irregularities in TI	Other Effects on TI
Control Points	Increasing the number of control points – fewer pockets and a smoother boundary	The depth of the control points determines the global shape of the contact. The remaining parameters control behavior between control points (drill holes).
Magnitude of values in drill holes	Increased magnitude of positive or negative values – fewer pockets and a smoother boundary	
Applying a skin to the entire model	Reduces pockets and smoothes the boundary. Increasing the magnitude of the values assigned to the skin will further reduce pockets and smooth the boundary.	Constrains the boundary to edges of the model where the user has inputted the 0 boundary in the form of conditioning data.
Use a skin above and below the model	Reduces pockets and smoothes the boundary. Increasing the magnitude of the values assigned to the skin will further reduce pockets and smooth the boundary.	Does not constrain the boundary at the edges of the model
Variogram range	Increasing the variogram range will reduce pockets and smooth the boundary.	
Variogram anisotropy	Increasing the range in the vertical direction creates larger vertical deviations in the boundary	
Variogram structure	Higher correlation – fewer pockets and a smoother boundary	
Including a nugget effect	Increased number of pockets and a more erratic boundary.	**Will result in boundaries that are not continuous.**
Degree of smoothing: MAPS	More smoothing reduces the randomness generated by SGS.	
Number of MAPS iterations	More iterations – fewer pockets and a smoother boundary	

The following TIs were generated with the above methodology to show the variety of features possible in the final TI. Many of the parameters described in Table 4-1 are redundant and are used to control the smoothness of the boundary: this can be visualized with Figure 4-10. Figure 4-11 shows the effect of adding a skin of conditioning data to the simulation. Figure 4-12 shows how the smoothing can be varied to generate TIs that have increased randomness.

Only XZ slices that show the boundary in cross section will be presented to conserve space. The TIs shown in Figure 4-10, Figure 4-11 and Figure 4-12 are 200x200x40 with unit block sizes.

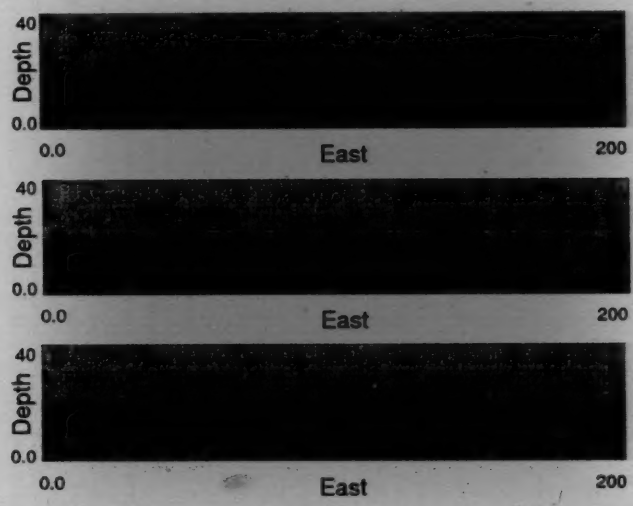

Figure 4-10: Effect of increasing the variogram range on weathered TIs. Control points have a spacing of 20 units. Variogram ranges shown are: Above – *ah1*=*ah2*=10, *avert*=5. Middle – *ah1*=*ah2*=20, *avert*=10. Below – *ah1*=*ah2*=60, *avert*=20. The search distance for each direction equals the range parameters. A minimum of 4 and maximum of 16 conditioning data were used in the simulation with 12 simulated nodes. Light gray – laterite. Dark gray – saprolite. Each block has unit width.

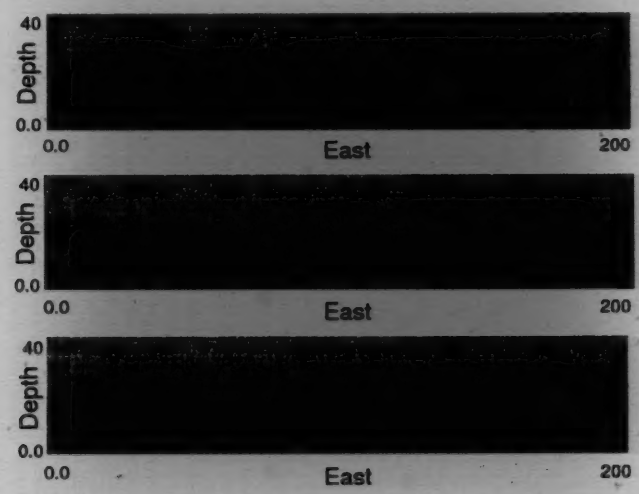

Figure 4-11: Effect of using different conditioning data options on the weathered TIs. Conditioning can be added around the edges of the model. Above – no boundary conditions (taken from Figure 4-10). Middle – normal scored data of magnitude 5 is added to the top blocks and -5 to the bottom blocks. Below – a skin around the entire model increases smoothness and constrains the boundary at the edges of the model. Light gray – laterite. Dark gray – saprolite. Each block has unit width.

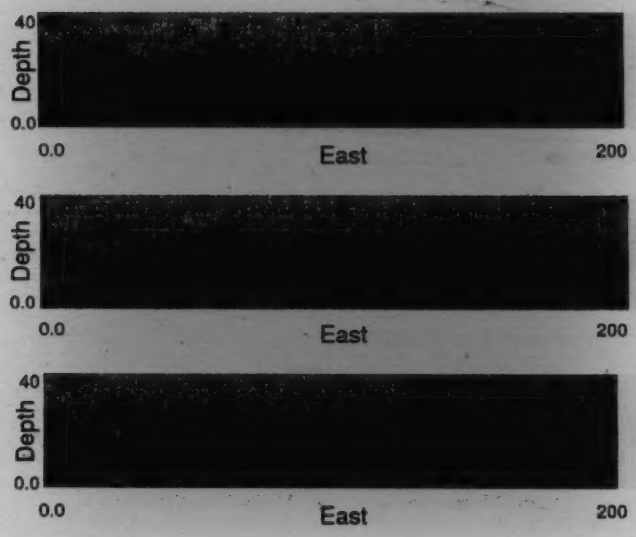

Figure 4-12: Effect of different smoothing options on weathered TIs. Increasing levels of smoothing from the upper TI to the lower. Light gray – laterite. Dark gray – saprolite. Each block has unit width.

4.4. Discussion

The geological realism of the TIs will be judged by a visual comparison with the photograph of a weathered contact presented in Chapter 1. The similarities between the TI and the coded photograph in Figure 4-13 are encouraging. The irregular nature of the contact and the distribution of pockets throughout both layers are apparent. The vertical fingers of laterite creeping into the saprolite, and vice versa, are also captured.

Figure 4-10, Figure 4-11, and Figure 4-12 give some examples of the versatility of this technique and Figure 4-13 shows that the TIs generated contain realistic features of actual deposits. There are many controls that allow for different types of boundaries to be defined to match site specific conditions. This gives the geostatistician a large degree of freedom when generating a TI. Moreover, it is possible to incorporate exploration data into this process. Rather than using pseudo drill holes as control points, actual exploration drill holes can be used. This would generate TIs that match the known site specific depth to contact at each drill hole location. These models could be used directly as the facies model for the weathered deposit.

Figure 4-13: Comparison of a TI with a weathered contact. Above – photograph of a weathered contact with the authors' interpretation of the contact, see Chapter 1 (modified from Bardossy and Aleva, 1990). Middle – photograph of the weathered contact recoded to laterite and saprolite categories to aid in comparison. Below – TI generated using proposed methodology, the model is 40 blocks by 200 blocks. Each block has unit width. Light gray – laterite. Dark gray – saprolite.

Chapter 5: Selecting Appropriate Training Images

Selecting a TI that is representative of the deposit or reservoir of interest is essential for an effective application of multiple point statistics. Methodologies that produce possible TIs, as presented in Chapters 3 and 4, generate TIs that are exhaustive and contain the desired geological features. However, these techniques generate many TIs with different properties such as different facies proportions, structures, directions of anisotropy, etc. When presented with a host of potential TIs, the geostatistician must decide which are more appropriate for their area of interest. Significant differences between the spatial statistics of local conditioning data and a TI may lead to artifacts in multiple point statistics (MPS). Often TI selection is done subjectively based on the available geological knowledge. While expert judgment is important, the methodology presented here attempts to augment the subjective aspects of selecting a TI by comparing the multiple point statistics of TIs to the available exploration data. There are insufficient exploration data to infer all multiple point statistics but there is often a sufficient number of data to make an accurate comparison between potential TIs and the data. This can be used to rank TIs on their similarity to the deposit of interest, thus helping to select a TI that is representative of the area of interest.

A methodology is presented that compares the multiple point statistics from available exploration data to the same statistics in TIs. The difference in the multiple point statistics can be used to select the TI that is most representative of the data set. This methodology is tested by taking simulated drillholes from the vein type TIs generated in Chapter 3 and comparing the drillhole statistics to the statistics of the parent TIs.

The fluvial and deepwater TIs described in Chapter 2 are compared to a data set provided by Chevron (data received from personal contact with Michael Pyrcz, Chevron) to demonstrate the methodology. It is intended that this methodology be used after the set of TIs has been narrowed based on the available geological knowledge. Lower order statistics, such as the variogram, should also be used when selecting a TI. This is commonly done and is not considered here, only the multiple point statistics are used to demonstrate the proposed methodology. An extension of this technique is to use the multiple point comparison to rank realizations. To demonstrate this, 30 multiple point realizations are generated using single normal equations simulation (SNESIM) and compared to 30 realizations generated using sequential indicator simulation (SIS). The realizations are then ranked based on their similarity to the parent TI and it is found that the multiple point realizations are more similar to the original TI. It is anticipated that ranking realizations will be applied to detect algorithm implementation problems and to

select appropriate realizations for further analysis, such as flow simulation, uncertainty calculations, or reserve estimation.

5.1. Proposed Methodology

The proposed methodology is a comparison of the absolute difference between the runs distribution or multiple point histogram of the TIs and the available exploration data. TIs are then ranked based on this difference. A detailed methodology follows: Section 5.1.1 describes the methodology for using the runs distribution to select TIs and Section 5.1.2 explains how the multiple point histogram can be used to rank TI.

Only one dimensional multiple point statistics are considered because well data and drillholes contain many samples in the vertical direction. As a result, any multiple point statistic used to compare TIs and exploration data will be better informed in the vertical direction.

Following the selection of an appropriate TI, the concept of ranking realizations using the multiple point histogram or the distribution of runs is explored.

5.1.1. Using Runs to Select TIs

Once the cumulative distribution of runs, see Chapter 1, is calculated for the available exploration data, it can be compared to the distribution of runs for all potential TIs. Comparison is based on the absolute difference between the distributions and summing over all runs lengths, see Figure 5-1.

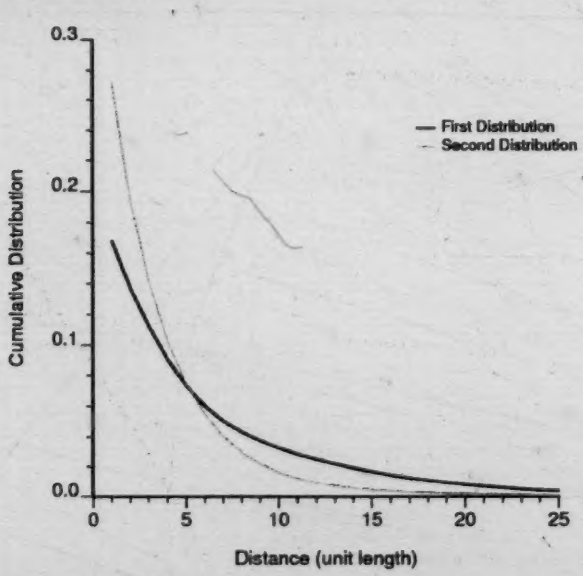

Figure 5-1: The difference between two runs distributions. For every length of runs the absolute difference is calculated and summed.

The difference between distributions may be calculated as:

$$diff = \sum_{l=1}^{n} \left| f_l^{*} - f_l^{**} \right| \qquad [5\text{-}1]$$

where *diff* is the difference between the distributions, l is the length of runs, n is the maximum length of runs, f_l^{*} is the cumulative frequency of the drill holes for a runs length of l and f_l^{**} is the cumulative frequency of the TI for a runs length of l. The smaller the summed difference, the more alike the two runs distributions. This gives a quantitative measure that can be used to rank potential TIs.

There are a number of practical issues with using the runs distribution to select TIs. First, the scale of the features in the TI may be much larger or smaller than the scale of features in the available data. This can be corrected by downscaling the TI or generating new TIs with the appropriate dimensions. The second issue arises from the distribution of runs being continuous. For example, a runs length of 100 would be very similar to a runs length of 99. If the absolute difference between runs lengths were calculated this would artificially inflate the difference between the distributions. This is dealt with by fitting an exponential function to the local runs distribution when calculating the difference, smoothing out the effect of similar runs lengths. Moreover, using the cumulative distribution of runs also minimizes this problem as a runs length of 100 would contain two 99 runs. A third practical consideration is the definition of the facies in the TI and the exploration data. The scanned image shown in Chapter 2 is used to demonstrate the effect of changing facies definitions. In general, using fewer facies will increase the number of long runs in the image and reduce the number of shorter runs, see Figure 5-7. This emphasizes the need to have TIs with the identical facies definitions as the drill holes in order to make a consistent comparison of statistics. A binary net/non-net set of facies is chosen for consistency.

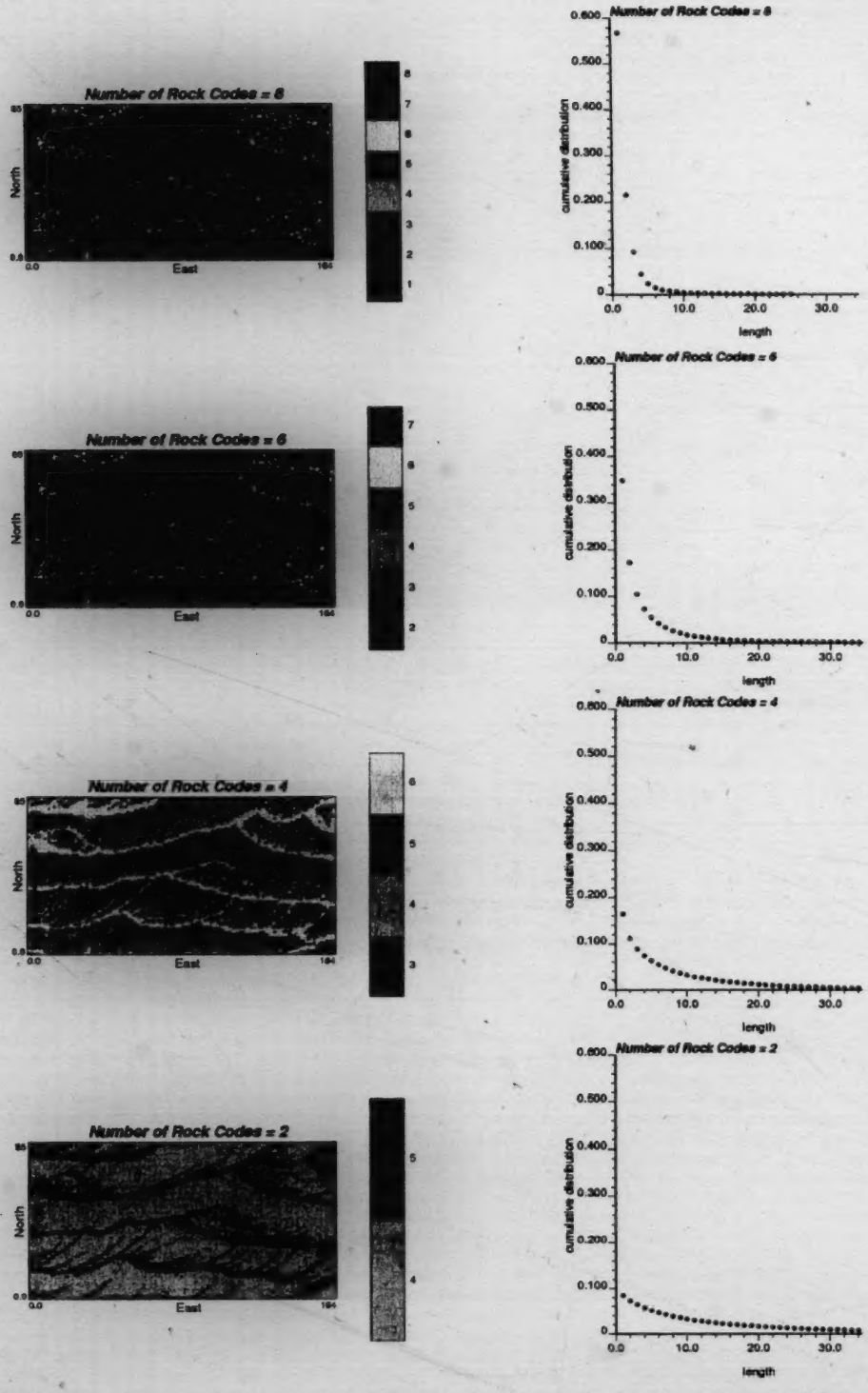

Figure 5-2: Map of combined rock codes (left) and associated distribution of runs (right). Each block has unit width.

5.1.2. Using the Multiple Point Histogram to Select TIs

A similar approach is taken to compare potential TIs to data based on the multiple point histogram. The methodology is identical to using the runs distribution but the difference is taken as the sum of the absolute difference between each multiple point bin.

When using the multiple point histogram to compare distributions an exponential fit is not used, as the multiple point histogram is not continuous and adjacent bins are unrelated. One implementation issue when using the multiple point histogram is dealing with the uninformed bins. Uninformed or zero bins, often pose a problem in multiple point statistics as they can be missing, not necessarily zero. It is often the case that a particular bin is not informed because of the sparse exploration data available, as opposed to the particular configuration the zero bin corresponds to actually occurring with zero frequency in the reservoir. Hence, two cases can be considered: 1) the naïve difference between the multiple point histogram, and 2) only summing the difference between bins when both bins are informed, effectively ignoring the zero bins that occur in the well data.

Case 1) naïve difference:

$$diff = \sum_{i=1}^{n} \left| f_i^{*} - f_i^{**} \right| \qquad [5\text{-}2]$$

Case 2) ignore zero bins:

$$diff = \sum_{i=1}^{n} \begin{cases} if\ f_i^{*} = 0, & 0 \\ if\ f_i^{**} = 0, & 0 \\ otherwise & \left| f_i^{*} - f_i^{**} \right| \end{cases} \qquad [5\text{-}3]$$

where *diff* is the difference between the distributions, i is the bin number, n is the maximum number of bins, f_i^{*} is the frequency corresponding to bin i for the wells and f_i^{**} is the frequency corresponding to bin i for the TI. The smaller the summed difference, the more alike the two multiple point distributions. In case 2, the difference at each bin is only summed if f_i^{*} and f_i^{**} are informed. Figure 5-3 shows two multiple point distributions for a square 4 point template.

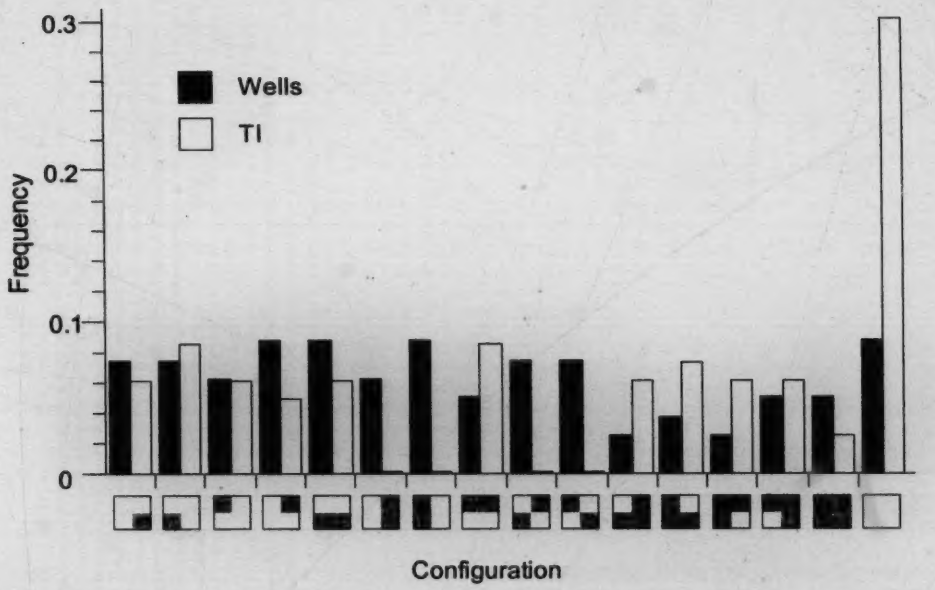

Figure 5-3: Comparing two multiple point histograms. Distributions are fabricated for illustrative purposes.

For the example shown in Figure 5-3 the difference between the frequencies for all 16 configurations would be summed to obtain the difference in the multiple point histogram. Note the four zero bins in the TI, for considering case 2, the difference would be calculated ignoring these bins.

The same categories must be present in all TI's and exploration data. Multiple point histograms generated with different number or types of categories would not be consistent and could not be compared.

5.1.3. Example: Selecting Vein Type TIs For Pseudo Drillhole Data

Five areas were selected from a flow simulation of Srivastava's fracture model, see Figure 5-4. The TIs were generated following the methodology presented in Chapter 3. The areas are 200x200x80 blocks and all have similar directions of anisotropy. In order to obtain other directions of anisotropy the TIs are rotated. Fifteen TIs can be obtained by considering each of the five areas in the xy, yz, and xz directions. For example, the xy image is 200x200x80, the yz image is 200x80x200 and the xz image is 80x200x200, see Figure 5-5. Drillholes are simulated by extracting columns of the TIs.

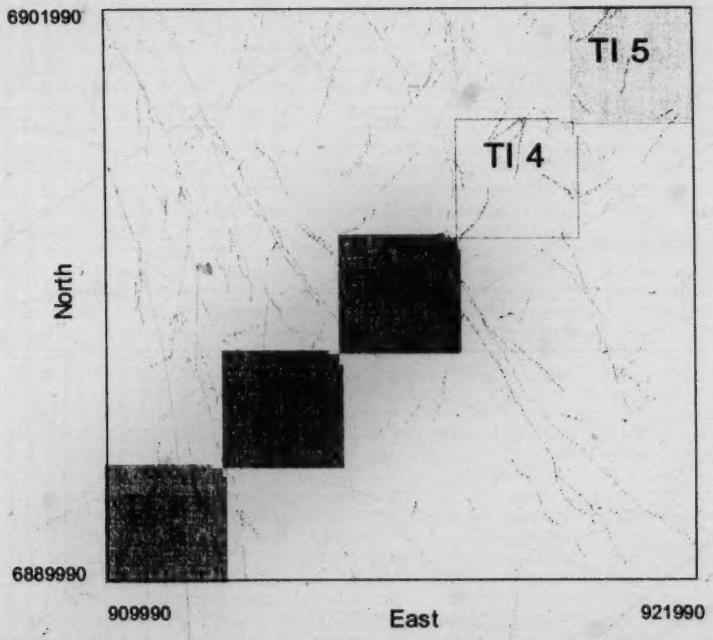

Figure 5-4: A typical slice of the fault model showing the location of the five TIs. Each block has a size of 15 units.

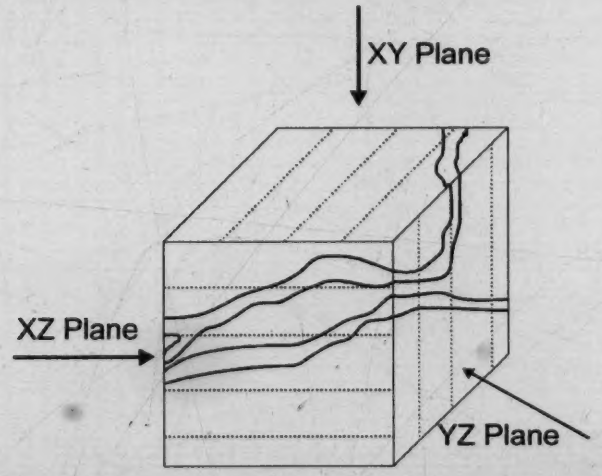

Figure 5-5: Orientation of TIs. Three different TIs can be created from each area by considering the one dimensional statistics in three different directions. Similarly, three sets of drillholes can also be obtained. NTS.

The goal is to calculate a summary statistic for the simulated drillholes and the TIs that will be able to match the drillholes to their parent TI. This would be analogous to having a set of drillholes and attempting to choose the most appropriate TI. In this case, the ideal TI is known and should be ranked high by the summary statistic.

As described above, 15 TIs were created by considering the 5 areas in the three principal directions. Drillhole sets consisting of 10, 50, 100 and 200 dill holes were extracted from all 15 TIs to assess the effect the number of drillholes has on selecting an appropriate TI.

Two measures of the ability of the runs distribution and the multiple point histogram to correetly select the appropriate TI are considered. First, a naive view: a count of the number of times that the incorrect TI was selected as the ideal image. This count of mislabeled TIs gives an indication of how well the drillhole sets were paired with their original TIs. Secondly, a more forgiving measure ranks all of the TIs for each drillhole set and assigns a penalty based on the rank of the parent TI.

$$Penalty = (Rank\text{-}1) \qquad [5\text{-}4]$$

This penalty is zero if the parent TI is most similar to the drillhole set (rank=1) and assigns an increasing penalty the further away the correct TI is ranked. This is repeated with all 15 drillhole samples from the 15 TI. Recall that four drillhole sets were taken from each TI with a different number of drillholes (10, 50, 100, and 200). A perfect score for the number of mislabeled TIs and penalties would be 0, with a maximum score of 15 and 225 respectively as the penalties are summed for each TI in each drillhole set size.

How well runs and the multiple point histogram selects the correct TI can be measured by the average number of incorrectly selected TI in the 15 TI/drillhole pairs for 25 randomly drawn drillhole sets. Each TI is ordered according to the difference measure, either runs or the multiple point histogram, and the penalty is calculated. This penalty is summed for all 15 TI/drillhole pairs and averaged over the 25 sets, see Figure 5-6.

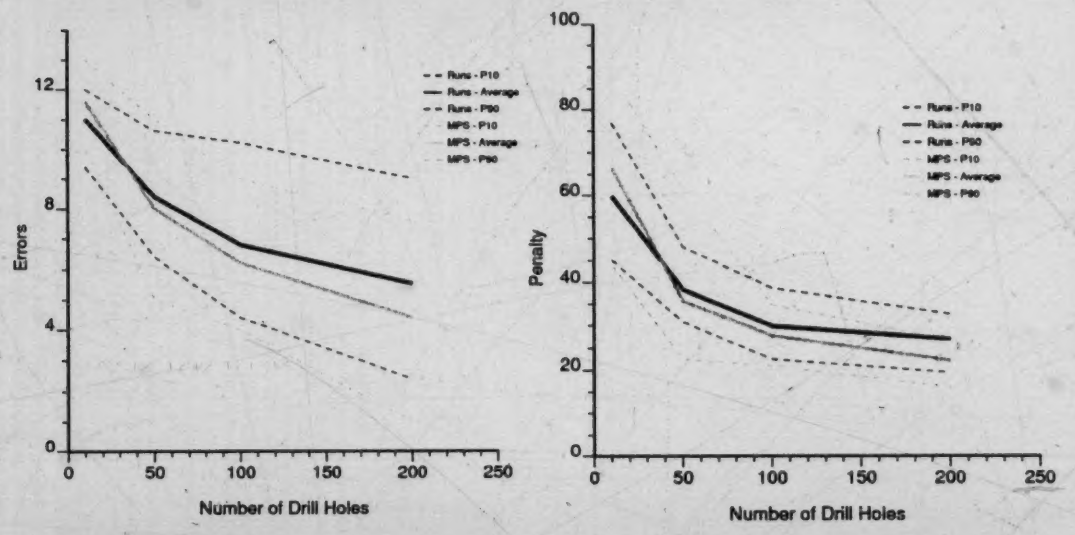

Figure 5-6: Comparing the runs distribution with an exponential fit to using the multiple point histogram including the zero bins. There is no significant difference when the zero bins are ignored. The error represents the count of the number of TI that were selected incorrectly. The penalty is defined by equation 5-1.

5.1.4. Discussion

There is very little difference when using the different options available for the runs or the multiple point histogram comparison. Using the naïve difference is similar to using an exponential fit (for runs) and ignoring the zero bins (for the multiple point histogram). Because the drillholes originated from the TIs used for comparison, it is reasonable that the runs lengths in the drillhole samples were similar to the TIs; therefore, considering an exponential fit to nearby runs will not provide significant gains. In reality, drillholes do not come from known TIs and it is suspected that the exponential fit would have larger benefits with actual data. Ignoring the zero bins for the multiple point histogram may not have improved performance for a similar reason. Because the drillholes originated from the TIs, it is impossible to have a zero bin in the TI without the corresponding bin in the drillholes being zero. With real data there is likely more inconsistency between the zero bins, increasing the importance of how the zero bins are handled.

Comparing the ability of runs and the multiple point histogram to select the correct TIs, it can be seen that for a small number of drillholes, runs perform better with a lower average penalty/errors and a lower spread in uncertainty, as seen in the p_{10} and p_{90} in Figure 5-6. When more data is available the multiple point histogram quickly becomes superior in correctly classifying the drillholes. This is expected as the multiple point histogram can contain more information than the runs distribution when properly informed but the multiple point histogram requires more data to be properly informed where as the runs distribution is more robust for sparse data.

5.2. Case Study: Chevron Data

5.2.1. Selecting TIs for Chevron Data

Chevron provided a data set consisting of 32 wells from a West African reservoir. The depositional environment of the reservoir is deepwater, which helps to narrow the selection of a TI. TIs from the fluvial/deepwater library (Pyrcz and Deutsch, 2003) are compared to the 32 wells using the methodology presented above. Three TIs Chevron selected as being representative of the area are included in the comparison. It is important that the facies for all TIs and the data are consistent. The TIs and Chevron data were converted to net and non-net categories for consistency as they contain different facies definitions. For the fluvial TIs in the training image library, the flood plain and abandoned channel fill categories were considered to be non net and the remaining categories net.

The 294 TIs from the fluvial/deepwater TI library (Pyrcz and Deutsch, 2003) and the three TIs from Chevron are compared to the Chevron data set. Each Chevron TI is 78x59x116 and modeled after a deepwater setting characterized by channels and lobes, see Figure 5-7. The distribution of runs for the TIs provided by Chevron are shown in Figure 5-8. Each TI in the fluvial/deepwater TI library is 256x256x128. The 32 wells have a net to gross ratio (NTG) of 0.49. As such, only TIs that have a NTG between 0.49 ± 0.15 are considered. There are 107 TIs that have a NTG in the acceptable range.

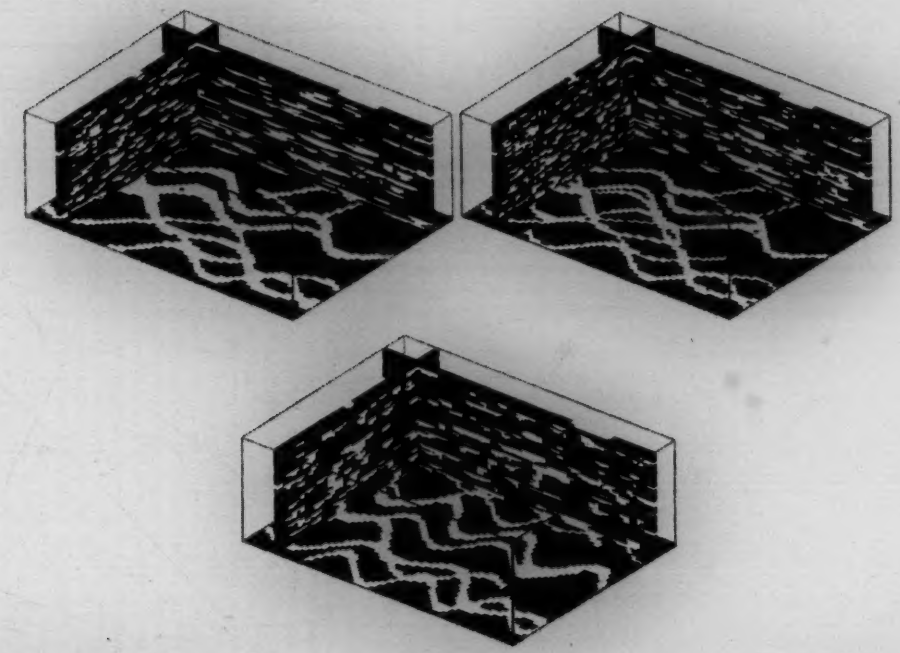

Figure 5-7: Three TIs received from Chevron, hereafter referred to as TI1 (top left), TI2 (top right), and TI3 (bottom). The facies are reduced to net/non-net categories for comparison. The black facies is considered non-net while the other facies are combined to form the net category. NTS but 3x vertically exaggerated.

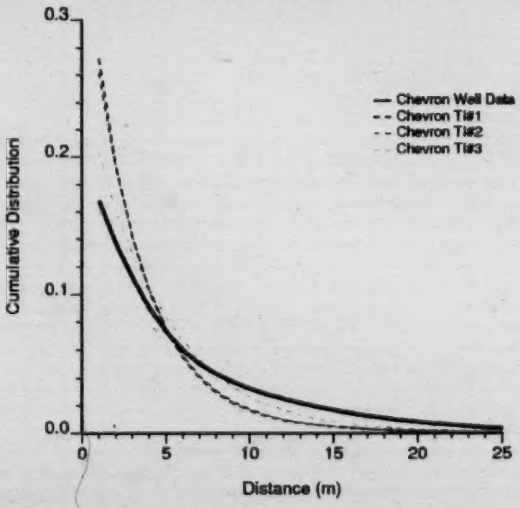

Figure 5-8: Runs distribution for the Chevron TIs.

The 107 of the total 297 TIs are ranked according to the differences in the runs distribution and the multiple point histogram, see Figure 5-9. It is known that the 32 wells originated from a deepwater setting, thus, it is expected that the deepwater TIs would be ranked higher. This is the case for ranking with the runs distribution and ranking with the multiple point histogram.

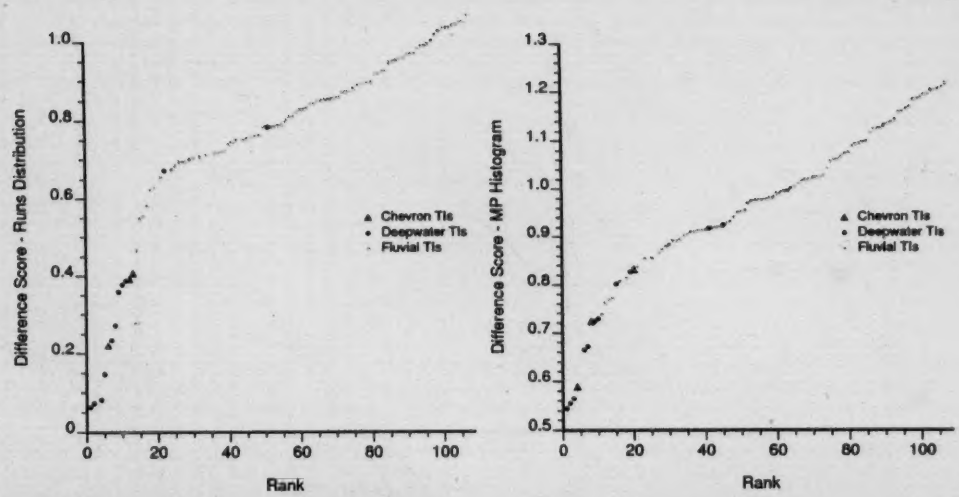

Figure 5-9: Comparing the TIs to the Chevron well data. Both the multiple point histogram and the distribution of runs are used to rank the TIs.

When the multiple point histogram is used to rank the TIs, ten of the top ten ranked TIs are from a deepwater setting, with two being the Chevron TIs. When the runs distribution is used to rank the TIs the top 29 are from a deepwater setting with three being the Chevron TIs. This is promising as the methodology has selected the correct depositional setting. It is also encouraging that the TIs that were selected by Chevron rank highly as these were deemed representative of the well data.

Figure 5-10 shows that in general, the ranking statistics agree well with each other. The high rank correlation, 0.9, observed between the two ranking methods is encouraging and would reinforce the selection of a particular TI.

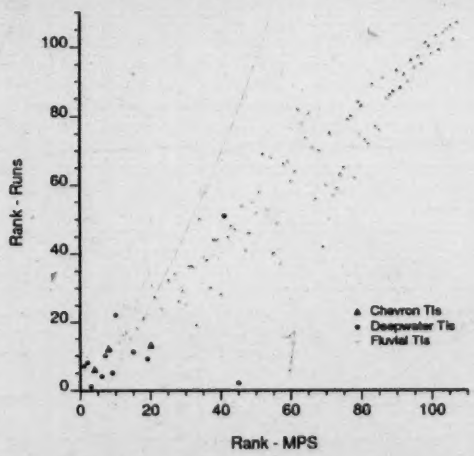

Figure 5-10: Cross plot of the score received by each TI. Rank correlation = 0.90.

Comparing multiple point statistics is a useful tool in helping to select TIs but a visual comparison of the TIs to the well data would further reinforce the selection of a TI. It is difficult to compare a large model, such as a TI, to well data; therefore, 32 vertical pseudo wells were drilled into each TI and are displayed in Figure 5-11 so that a visual comparison to the 32 wells provided by Chevron can be made. Shown are the highest and lowest ranked TIs using the ranking methods presented above, as well as, the three TIs provided by Chevron.

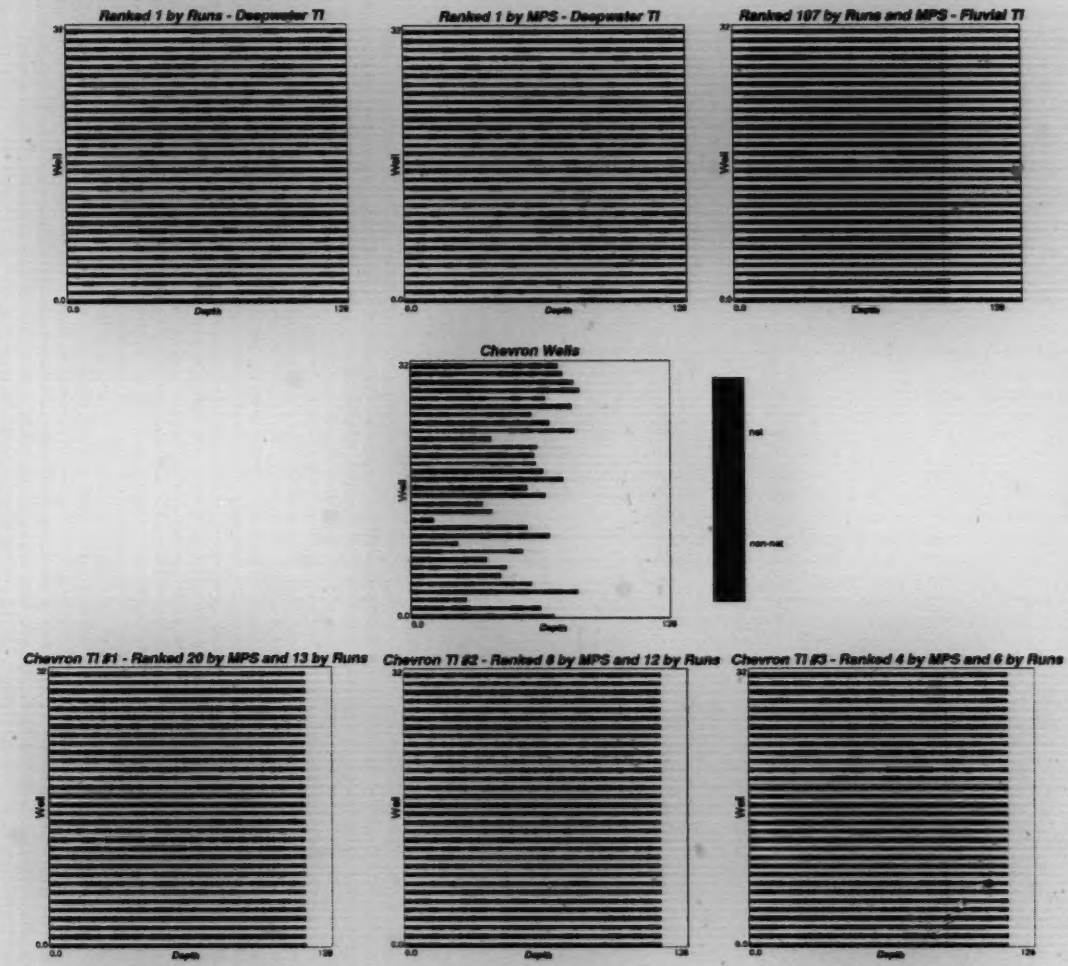
Ranked 1 by Runs - Deepwater TI
Ranked 1 by MPS - Deepwater TI
Ranked 107 by Runs and MPS - Fluvial TI
Chevron Wells
Chevron TI #1 - Ranked 20 by MPS and 13 by Runs
Chevron TI #2 - Ranked 8 by MPS and 12 by Runs
Chevron TI #3 - Ranked 4 by MPS and 6 by Runs
Well
Depth

Figure 5-11: 32 wells from the highest and lowest ranked TIs. Wells are taken from the TIs as columns of the TI. Both runs and MPS ranked the same TI 107th. The 3 Chevron TIs are also included. Layout of the figures is such that a visual comparison can be made between the well data and the ranked TIs. All wells are assumed to be vertical. Each well section has unit length.

5.2.2. Discussion: Using MPS to Select TIs

Selecting TIs based on a multiple point statistical comparison is meant to narrow the list of possible TIs. It is important to understand the role of the runs distribution and the multiple point histogram in selecting TIs. From Section 5.1.3 it is believed that runs are

more stable for sparse data while the multiple point histogram does well when there is sufficient data to inform the bins. Each well in the Chevron data contains an average of 118 categorical assignments for a total of 3773 data points. This should be a sufficient number of data to generate a multiple point histogram that would outperform the runs distribution for TI selection. If there are too few wells and inference of the 1D multiple point histogram is not possible, runs would likely be more robust. Both statistics should be used to help select TIs.

The final selection should be made on the bases of all available information including the NTG ratio, histogram, variogram, geological knowledge, and experience with similar formations. It has been common practice to use these sources of information to select TIs, however, the methods to compare TIs and exploration data are usually subjective. It has been shown that multiple point statistics can be calculated on exploration data, such as the runs distribution or the multiple point histogram and that comparing these statistics to the suite of available TIs helps to narrow the choice of TI and provide objective support for TI selection.

5.2.3. Realization Ranking with MPS

The same methodology that is used to compare exploration data to TIs can be used to compare geostatistical realizations to their parent TIs for model validation. The multiple point statistics are compared as per the methodology given above. This is demonstrated by comparing realizations generated using SNESIM (Strebelle, 2002) to their parent TI, Chevron TI#3. For comparison, realizations were also generated using sequential indicator simulation (SIS) with the variogram taken after Chevron TI #3. TI #3 was selected because it was ranked highly by both the multiple point histogram and the runs distribution.

All realizations generated are 78x59x50 with 75m 75m and 6m block sizes respectively, and are conditioned to the 32 wells provided by Chevron. This only covers the lower half of the data set to reduce the time required to generate the realizations. TI #3 (see Figure 5-12) is used for both SNESIM (Strebelle, 2002) and SIS to attempt to reproduce the multiple point features of the TI.

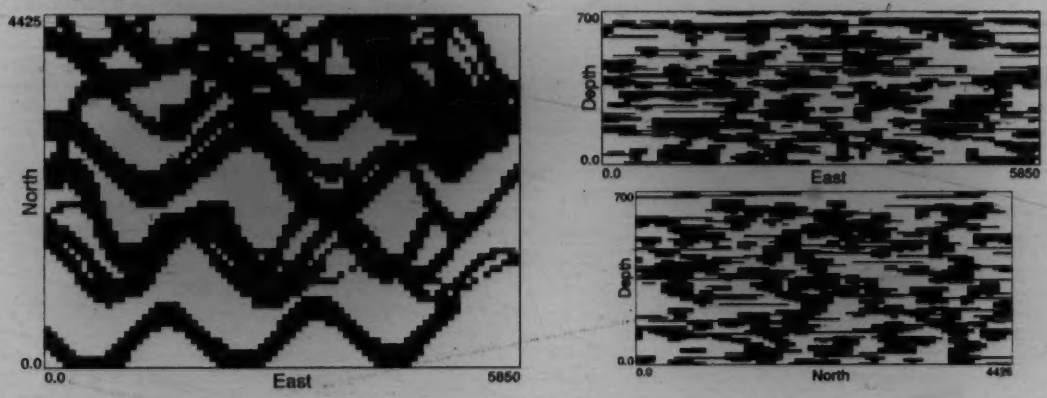

Figure 5-12: Left – plan view of Chevron TI #3. Right - cross sections of Chevron TI #3. The vertical direction is exaggerated. Black is net. Each block has unit width.

5.2.4. Generating Realizations: SNESIM

Strebelle's (2002) SNESIM algorithm for multiple point stimulation is applied to generate realizations that attempt to honour the multiple point statistics of the TI shown in Figure 5-12. This algorithm uses the single normal equations, rather than an iterative approach, to create geostatistical realizations. The reader is referred to Strebelle (2002) for a more detailed description of the methodology.

Thirty realizations were generated using a 50 point multiple point template. The template is a three dimensional irregular template determined using the optimized template selection methodology presented by Lyster and Deutsch (2006b). The parameters used in SNESIM are: a maximum of 16 conditioning data; a minimum of 10 data events; 4 search trees; and a search large enough to find 16 conditioning data at all locations. Figure 5-13 shows a typical realization.

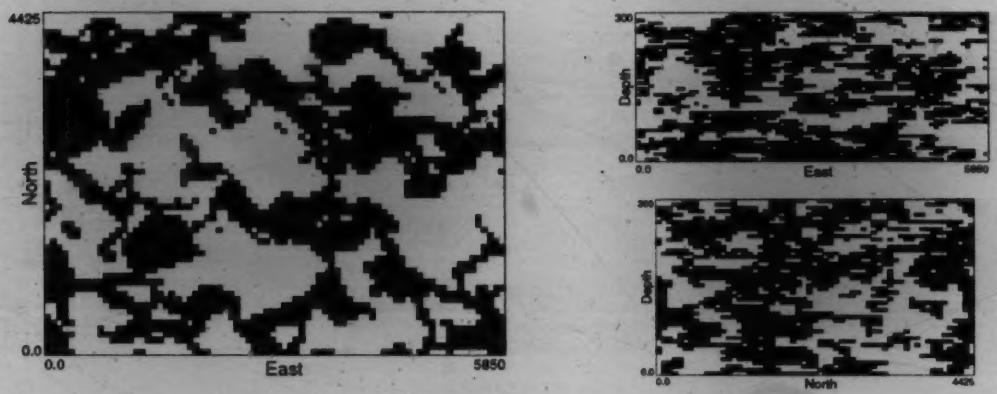

Figure 5-13: Typical SNESIM (Strebelle, 2002) realization. Left – plan view. Right - cross sections. The vertical direction is exaggerated. Black is net. Each block has unit width.

5.2.5. Generating Realizations: SIS

The goal is to use SIS to generate realizations that contain the same features as TI#3; therefore, the variogram calculated from the TI is used to create 30 SIS realizations, see Chapter 1 for a definition of the *sph* variogram structure:

$$\gamma(\mathbf{h}) = 0 + 0.1 sph_{\substack{ah1=15 \\ ah2=14}}(\mathbf{h}) + 0.0626 sph_{\substack{ah1=50 \\ ah2=45}}(\mathbf{h}) + 0.075 sph_{\substack{ah1=300 \\ ah2=60}}(\mathbf{h}) \qquad [5\text{-}5]$$

where *ah1* is in the 90° direction, *ah2* in the 0° direction, and *av* is the vertical direction. One SIS realization is shown in Figure 5-14.

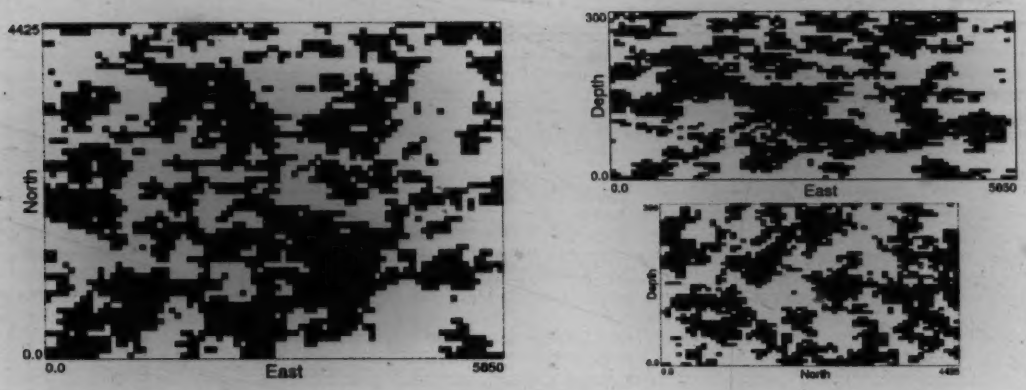

Figure 5-14: Typical SIS realization. Left – plan view. Right - cross sections. The vertical direction is exaggerated. Black is net. Each block has unit width.

Figure 5-15 shows that the realizations generated using SIS reproduce the variogram for the TI, with a slightly lower correlation in the horizontal directions. However, it is clear that the nonlinear structure seen in the TI, Figure 5-12, is missing. This is most noticeable in the horizontal slice, see Figure 5-14.

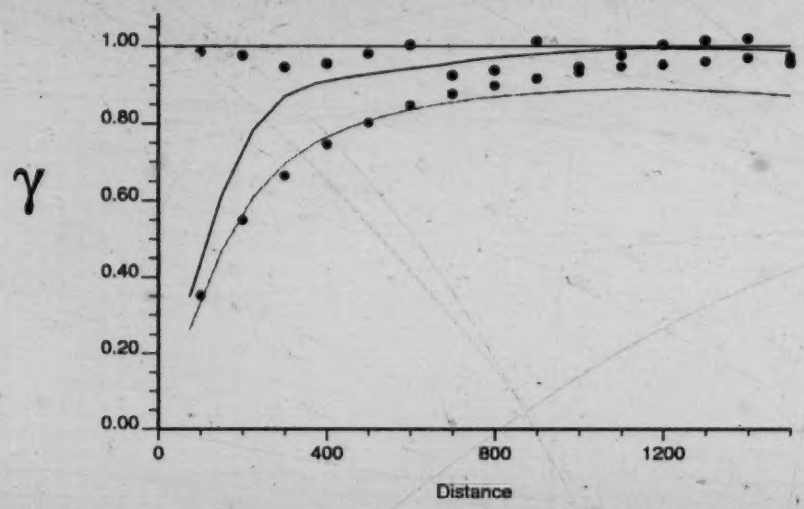

Figure 5-15: Comparing the variogram from the TI and one typical SIS realization. Dark gray represents the major direction of continuity (90°), black is the minor direction, and light gray is the vertical direction. Lines represent the variogram for the TI and the points are the variogram of a SIS realization.

5.2.6. Comparing Geostatistical Realizations to TIs

The 30 realizations generated using SIS and the 30 generated using SNESIM (Strebelle, 2002) are compared to the TI using the distribution of runs and the multiple point histogram.

The distribution of runs is considered to be a one dimensional statistic. Because most of the nonlinear features are apparent in the XY plane, see Figure 5-12, the runs difference was calculated for the X and Y directions and averaged to get the difference shown in Figure 5-16.

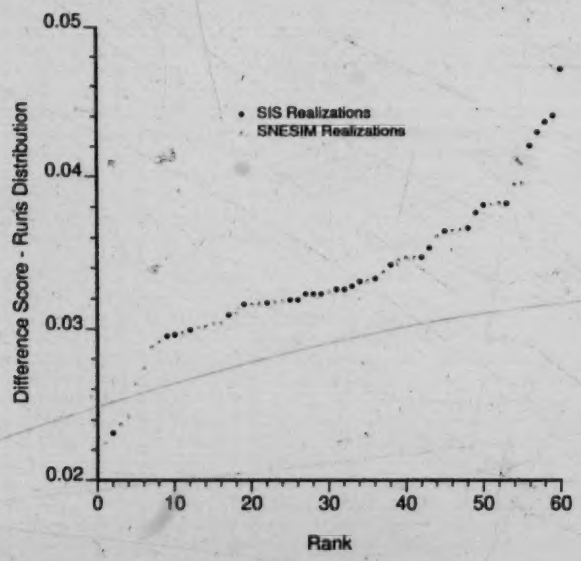

Figure 5-16: Ranking realizations based on the runs distribution.

The multiple point histogram was also used to compare realizations, see Figure 5-17. A 3x3x2 template was used. Note that this corresponds to $2^{(3x3x2)}$=262,144 bins and increasing to a 3x3x3 template results in 134,217,728 bins. Since there are only 212,268 possible 3x3x2 statistics in the realizations it is not practical to consider a template greater than 3x3x2 as the bins of the histogram would not be well informed.

The differentiation between the simulation techniques is obvious with the multiple point histogram. SNESIM generates realizations that are more similar to the original TI, in that the multiple point statistics are honoured. Comparing the ranking of the two measures, Figure 5-18 shows that they differ significantly. The measures are most noticeably different when ranking the top ten realizations, which are arguably the most important realizations.

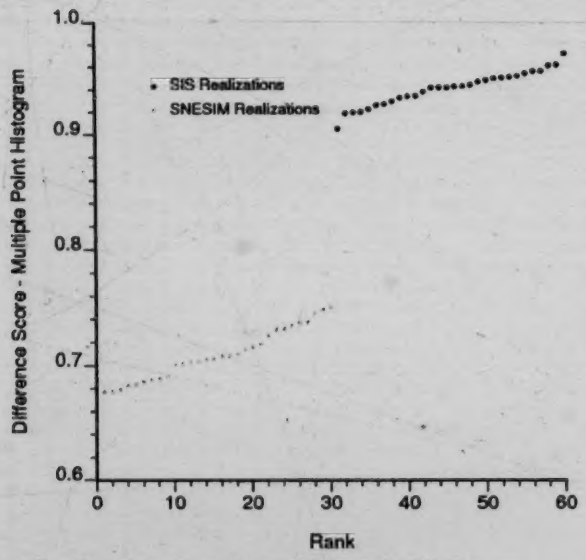

Figure 5-17: Ranking realizations based on the multiple point histogram.

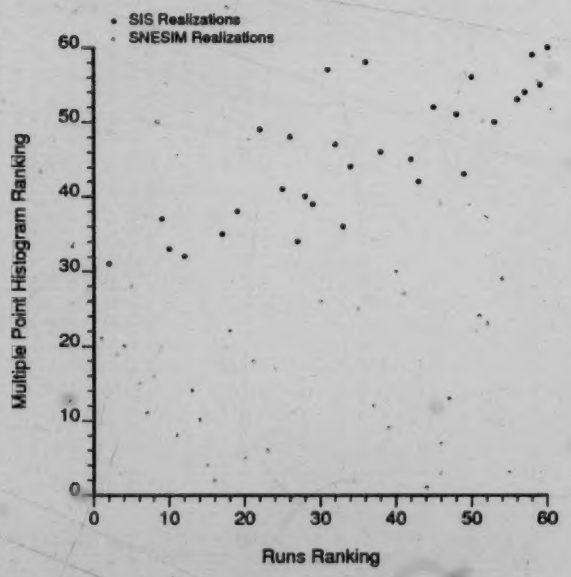

Figure 5-18: Comparing the two ranking measures. Rank correlation = 0.43.

5.2.7. Discussion: Using MPS to Rank Realizations

The selection of a statistic for ranking is extremely important. It is apparent that the multiple point histogram can better differentiate between the different simulation methods (especially between methods that reproduce multiple point statistics and those that do not). The visual inspection of the SNESIM realizations indicated they are more

similar to the TI, which supports the use of the multiple point histogram when ranking realizations. In this situation the runs distribution does not capture the difference between the SNESIM and SIS realizations. The multiple point histogram for a realization is well informed, as there are many repetitions of the template whereas, the runs distribution is to be used when there are sparse data and a well informed multiple point histogram is not attainable (e.g. statistics calculated from sparse exploration data). Therefore, the multiple point histogram is considered superior when ranking realizations relative to an exhaustive TI due to its increased information content.

In this example the ranking measures were used to show that the variogram cannot capture the nonlinear features of a TI, as shown by the higher ranking of the SNESIM realizations. It is expected that this would not be the main use for ranking realizations. In practice, this method would be applied to select the realizations that most resemble the original TI and to check for large differences between the multiple point statistics of the TI and simulated realizations. If multiple point simulation is used, it is assumed that the goal is to model nonlinear and ordering features that cannot be captured otherwise. Thus, this ranking measure can be used to determine which realizations have best reproduced the features borrowed from the TI (see Figure 5-19)

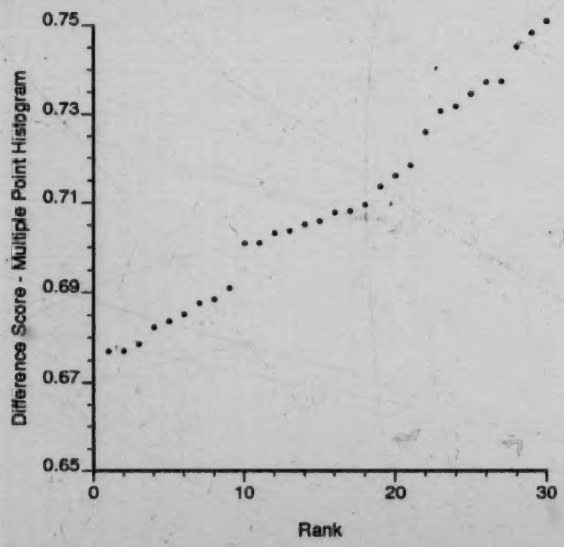

Figure 5-19: Ranking the 30 SNESIM realizations using the multiple point histogram.

Figure 5-19 shows that there is a difference between SNESIM realizations. The top nine realizations have a greater similarity to the original TI, see Figure 5-20. This could be used to determine which realizations to keep for future analysis. As shown in Figure 5-20, there is a significant visual difference between the realization ranked 30th and the highest ranked realization.

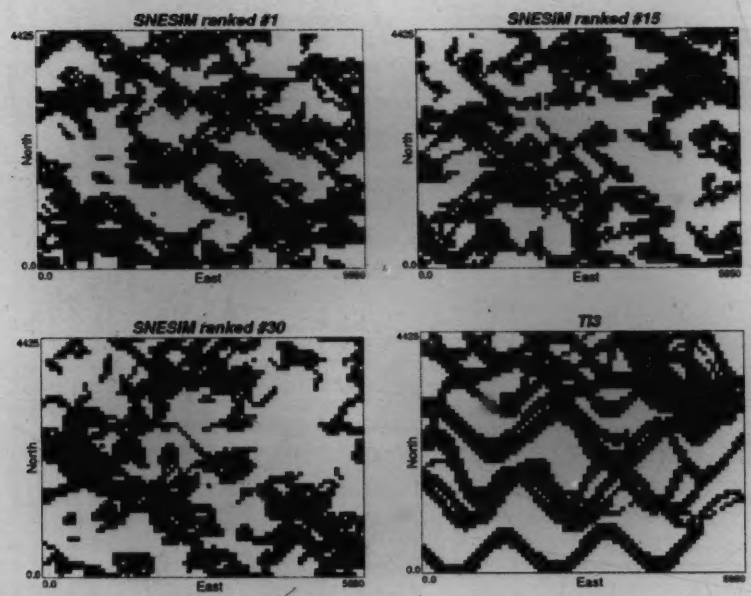

Figure 5-20: Plan views of ranked SNESIM realizations and the parent TI for comparison. Black is net. Each block has unit width.

On a cautionary note, this measure should not be used to determine which models represent the p10, p50 or p90 models. It should be utilized to highlight which realizations should be discarded as not capturing the features inherent in the TI. Realization ranking for the assignment of percentiles should be based on a transfer function.

Chapter 6: Conclusions and Future Work

6.1. Conclusions

The variogram has been extremely powerful in capturing the anisotropy seen in many deposits and reservoirs but it is becoming common to question the reliance of geostatistics on the variogram. The relative simplicity of the variogram and the ability to infer its structure from sparse data has contributed to its longevity. With this simplicity much important information is lost. The complex geometries seen in nature are reduced to three directions of anisotropy. MPS has been presented as the answer to the linear limitations of the variogram. MPS has the potential to capture the complex behaviors seen in geological formations.

As more sophisticated multiple point simulation algorithms that can accurately reproduce a given multiple point set are developed, attention should turn to what MPS are being reproduced. A poor variogram will produce poor geostatistical realizations and a poor set of MPS will produce poor multiple point realizations. The importance of representative MPS is key to a successful application of multiple point simulation. To be representative, the MPS require two features: 1) they must be geologically realistic, and 2) they must be appropriate for the area of interest.

There are insufficient exploration data to infer all necessary MPS and TIs have surfaced as the source of such statistics. The lack of TIs is a serious problem hindering the use of MPS in the mining industry. Due to the increasing use of MPS in the petroleum industry, there are emerging solutions to many MPS implementation problems. As such, the main obstacle preventing the use of MPS to capture curvilinear geological features of mineral deposits is the absence of TIs. This thesis has presented possible sources of realistic TIs in the form of: potential exhaustive data sets; process based approaches for vein type deposits; and a methodology to use SGS to generate realistic weathered profiles.

There are a number of data sets available that could be used as TIs. The most likely source of data for use as a TI would be a similar deposit that has been mined in the vicinity of the deposit of interest. Moreover, if a company has mined part of a deposit, the blasthole data from the mined out area could be used as a TI for future estimation of that deposit.

The use of a data set as a TI guarantees that the MPS used will be geologically realistic, trusting the data are reliable. Although, an exhaustive data set that is representative of

the deposit of interest is not often available. In this case, process based approaches can be used to mimic the geological formation of the deposit. This has been shown to generate realistic TIs for vein type deposits. It is not always necessary to mimic all processes that lead to the formation of the deposit. A pseudo genetic approximation of the process is often sufficient. Modeling the physical movement of the hydrothermal fluids, while ignoring the chemical reactions that are necessary for the formation of veins, produced realistic TIs. The precise geological processes that form mineral deposits are difficult to model and at times are unknown; however, geologically realistic MPS can still be inferred from TIs that do not consider the exact formation process if they have the same features and characteristics of mineral deposits.

The simple methodology provided here for weathered deposits shows that the generation of geologically realistic TIs for mineral deposit applications is possible with the tools currently available, such as SGS. In this case, SGS is used to generate the boundary between weathered layers. It should be noted that SGS is only used to generate TIs and that these TIs contain the desired nonlinear features that can then be reproduced with multiple point simulation algorithms.

There are many advantages to using the methodologies presented in this thesis for TI generation rather than using an exhaustive data set. The flexibility of the process based approach makes generating many TIs possible. Moreover, these TIs can be created in such a way as to contain the desired geological features rather than searching for a representative data set. This flexibility is useful during the TI selection process as it gives the geostatistician a number of potential TIs to select. However, eventually a choice of TI must be made and this can be unduly subjective. Comparing exploration data to potential TIs is difficult. A methodology that ranks potential TIs based on their MPS has been shown to provide useful information for the choice of TIs.

There are a number of practical considerations that must be addressed when using MPS to compare two sets of data, whether for the comparison of exploration data with potential TIs or the validation of realizations against a TI. The first consideration is the scale of the features present; if the features are identical, but of a different size, the resulting comparison will show that the two sets of data are different. The second major consideration is which MPS to use. The multiple point histogram and the distribution of runs have been demonstrated; however, there are other MPS that could be used to compare data sets. The choice of statistic will directly impact which TI is selected or which realization is ranked highly. Thus, the statistic selected should be related to features that will impact the transfer function. A comparison between MPS is not sufficient evidence to select a TI, other sources of information must be used in conjunction with a statistical comparison, such as NTG, anisotropy, single point histogram and geological knowledge.

It has been shown that by using a multiple point statistical comparison, the correct geological setting was selected for the well data provided by Chevron. Moreover, the TIs that were selected by Chevron as being representative were also ranked highly by the

statistical comparison. This is strong evidence that there is important information gained by performing a simple calculation of the difference between two sets of data.

Ranking realizations is also a useful tool for determining which realizations contain the desired features present in the TI. In this context, it is recommended that the multiple point histogram be used as the ranking measure because exhaustive TIs and realizations provide sufficient datasets for reliable calculation of the multiple point histogram.

This thesis provides a variety of methodologies to generate TIs that are exhaustive and contain realistic geological features. This will provide the mining industry with the necessary tools to use MPS for facies modeling. Similar to selecting the appropriate variogram, the choice of TI is vital to the implementation of MPS. Objective ranking measures for potential TIs have been presented that have been shown to successfully rank TIs. This methodology can be extended to ranking multiple point realizations after a reasonable multiple point algorithm has generated realizations.

6.2. Future work

Multiple point statistics are a relatively new way of quantifying the uncertainty in reserves and still requires solutions to various implementation problems. This aside, before a successful application of MPS is possible, TIs that contain the desired curvilinear features of mineral deposits are needed. TIs for vein type deposits and weathered profiles are only a small fraction of the deposit types that require a set of TIs. Methodologies for other deposit types such as oil sands, porphyry, skarns, etc. would make available the option of MPS to more mining geostatisticians. Future research should not only be focused on solving the problems facing a successful workflow for MPS, but also directed at generating TIs that contain desirable features.

TIs were generated for vein type deposits from a given fracture model. There is much work to be done in the area of fracture modeling. Techniques to generate a realistic fracture model from a set of exploration data are required as the methodology presented here assumes that there is fracture model available for the area of interest. Fractures must be inferred from the available exploration data, outcrops, and geological knowledge. Incorporating these into a representative fracture model that can then be used to generate a realistic TI is an area that requires development.

With the methodologies developed for this thesis it is possible to compare the distribution of runs or the multiple point histogram. No other flexibility was considered. It would be useful to compare the single point histogram, variogram, NTG, transition probabilities, runs distribution, and the multiple point histogram. Extending this further, it would be possible to combine these multiple ranking methods by weighing each difference:

$$\textit{Difference score} = 0.2(\textit{variogram}) + 0.2(\textit{histogram}) + 0.3(\textit{runs}) + 0.3(\textit{multiple point histogram})$$

This would generate a difference score that would incorporate multiple sources of information. Weighting could be assigned based on importance. For example, if the

features are linear, less weight would be placed on the MPS. If there are sparse data and the multiple point histogram is not well informed and its weighting would be reduced. In this way, all available exploration data can be combined into one ranking measure.

Another area of work that was not explored involves developing new/different MPS that could be used for comparison. The connectivity function has been mentioned, but new measures could be developed specifically for comparing geological data.

Bibliography

Alsop, G. I., Holdsworth, R. E., McCaffrey, K. J. W., and Hand, M., (2004). Flow Processes in Faults and Shear Zones. London, Geological Society, Special Publications, 224 p.

Armstrong, M., Galli, A.G., Le Loc'h, G., Geffroy, F. and Eschard, R., 2003. Plurigaussian simulations in geosciences. Berlin, Springer, 149 p.

Arpat, G. B. and Caers, J., 2004. A multi-scale, pattern-based approach to sequential simulation, *in* Leuangthong, O. and Deutsch, C., eds., 7th International Geostatistics Congress. Banff, Canada, Springer p. 255-264.

Bardossy, G. and Aleva, G. J. J., 1990. Developments in Economic Geology 27: Lateritic Bauxites. Hungary, Elsevier, 624 p.

Bland, W. and Rolls, D., 1998. Weathering: An Introduction to the Scientific Principles. Oxford University Press, 271 p.

Caers, J., 2001. Geostatistical Reservoir Modeling Using Statistical Pattern Recognition. Journal of Petroleum Science and Engineering, 29 (3), p. 177-188.

Chilès, J. P., 1989. Three dimensional geometric modeling of a fracture network, *in* Buxton, B.E., ed., Geostatistical, Sensitivity and Uncertainty Methods for Ground-Water Flow and Radionuclide Transport Modeling. Columbus, Ohio, Battelle Press, p. 361-385.

Delvigne, J. E., 1998. Atlas of Micromorphology of Mineral Alteration and Weathering. The Canadian Mineralogist, Special Publication 3. Mineralogical Association of Canada. 494 p.

Deutsch, C. V., FLOWSIM: 1987. www.ualberta.ca/~cdeutsch/ accessed March 20, 2006.

Deutsch, C. V., 1992. Annealing Techniques Applied to Reservoir Modeling and the Integration of Geological and Engineering (Well Test) Data. PhD Thesis, Stanford University, Stanford, CA. 306 p.

Deutsch, C. V., 1998. Cleaning Categorical variables (lithofacies) realizations with maximum a-posterior selection. Computers & Geosciences, v. 24 (6), p. 551-562.

Deutsch, C. V., 2002. Geostatistical Reservoir Modeling. New York, Oxford University Press, 376 p.

Deutsch, C. V. and Tran, T. T., 2002. FLUVSIM: A program for object-based stochastic modeling of fluvial depositional systems. Computers and Geosciences, 28, p. 525-535.

Duke, J. H. and Hanna, P. J., 2001. Geological Interpretation for Resource Modeling and Estimation, *in* Edwards, A. C. ed., Mineral Resource and Ore Reserve Estimation – The AusIMM Guide to Good Practice. Melbourne, Australia, The Australasian Institute of Mining and Metallurgy, p. 147-156.

Faybishenko, B., Witherspoon, P. A., and Benson, S. M., 2000. Dynamics of Fluids in Fractured Rock. Washington, American Geophysics Union, 400 p.

Guardiano, F. and Srivastava, M., 1993. Multivariate geostatistics, Beyond bivariate moments, *in* Soares, A. ed., Geostatistics Troia '92. v. 1, p. 133-144.

Guilbert, J. P. and Park, C. F. Jr., 1996. The Geology of Ore Deposits. New York, W. H. Freeman and Company, 985 p.

Isaaks, E. H. and Srivastava, R. M., 1989. An Introduction to Applied Geostatistics. New York, Oxford University Press, 561 p.

Journel, A., 2004. Beyond covariance: The advent of multiple-point geostatistics, *in* Leuangthong, O. and Deutsch, C. eds., 7th International Geostatistics Congress. Banff, Canada, Springer, v. 1, p. 225-235.

Journel, A. G., and Huijbregts, Ch. J., 1978. Mining Geostatistics. New Jersey, The Blackburn Press. 600 p.

Lee, C. H., and Farmer, I., 1993. Fluid flow in Discontinuous Rocks. London, Chapman & Hall. 169 p.

Liu., Y, Harding, A., Gilbert, R. and Journel, A., 2004. A workflow for multiple-point geostatistical simulation, *in* Leuangthong, O. and Deutsch, C. eds., 7th International Geostatistics Congress. Banff, Canada, Springer, v. 1, p. 245-255.

Lyster, S. and Deutsch, C. V., 2006a. A New MPS Simulation Algorithm Based on Gibbs Sampling, *in* Leuangthong, O. and Deutsch, C., eds., Report Eight Center for Computational Geostatistics.

Lyster, S. and Deutsch, C. V., 2006b. An Entropy-based Approach to Establish MPS Templates, *in* Leuangthong, O. and Deutsch, C., eds., Report Eight Center for Computational Geostatistics.

Mood, A. M., 1940, The distribution theory of runs, The Annals of Mathematical Statistics, 11, p. 367-392.

National Research Council (NRC), 1996. Rock Fracture and Fluid Flow. Washington, National Academy Press, 551 p.

Ortiz, J. M. and Deutsch, C. V., 2004. Indicator simulation accounting for multiple-point statistics. Mathematical Geology, v. 36 (5), p. 545-565.

Pyrcz, M.J., Catuneanu, O. and Deutsch, C.V., 2005. Stochastic Surface-based Modeling of Turbidite Lobes, American Association of Petroleum Geologists, 89 (2), p. 177-191.

Pyrcz, M. J. and Deutsch, C. V., 2003. A Library of Training Images for Fluvial and Deepwater Reservoirs and Associated Code, *in* Deutsch, C., ed., Report Five Center for Computational Geostatistics.

Pyrcz, M.J and Strebelle, S., 2006, Event-based Geostatistical Modeling of Deepwater Systems, GCSSEPM 2006.

Robert, F. and Poulsen, H., 2001. Vein Formation and Deformation in Greenstone Gold Deposits, *in* Richards, J. P. and Tosdal, R. M., eds., Structural Control on Ore Genesis. Society of Economic Geologists Inc., p. 111-156.

Rossmanith, H. P., 1998. Mechanics of Jointed and Faulted Rock. Netherlands, A. A. Balkema Publishers, 658 p.

Sahimi, M., 1993. Flow phenomena in rocks: from continuum models to fractals, percolation, cellular automata and simulated annealing. Reviews of Modern Physics, v. 65 (4), p. 1393-1534.

Sinclair, A. J., and Blackwell, G. H., 2002. Applied mineral inventory estimation. Cambridge, Cambridge University Press, 381 p.

Srivastava, R. M., 2002. Nuclear Waste Management – Probabilistic Discrete Fracture Network Models for the Whiteshell Research Area. 181 p.

Strebelle, S., 2002. Conditional Simulation of Complex Geological Structures Using Multiple-Point Statistics. Math Geology, 34 (1), p. 1-22.

Strebelle, S. and Journel, A., G., 2000. Sequential simulation drawing structures from training images, *in* Kleingled, W. and Krige, D. G., eds., 6th International Geostatistics Congress, Cape Town, South Africa. Geostatistical Association of Southern Africa, v. 1, p. 381-392.

Takayasu, H., 1985. A deterministic model of fracture. Progress in Theoretical Physics, v. 74 (6), p. 1343-1345.

Zhang, T., Switzer, P. and Journel, A., 2004. Sequential conditional simulation using classification of local training patterns, *in* Leuangthong, O. and Deutsch, C. eds., 7th International Geostatistics Congress: Banff, Canada, Springer, v. 1, p. 265-275.